

MASTER

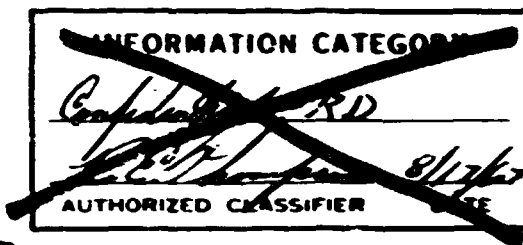
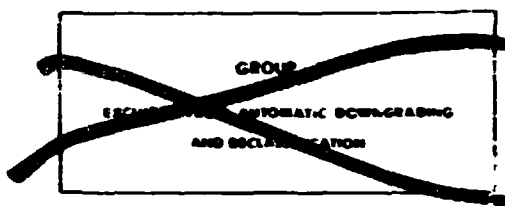
~~CONFIDENTIAL~~  
~~RESTRICTED DATA~~  
~~Dec 1964~~

Subcontract NP-1

NOTICE  
This report was prepared as an account of work sponsored by the United States Government. Neither the United States nor the United States Energy Research and Development Administration, nor any of their employees, nor any of their contractors, subcontractors, or their employees, makes any warranty, express or implied, or assumes any legal liability or responsibility for the accuracy, completeness, or usefulness of any information, apparatus, product or process disclosed, or represents that its use would not infringe privately owned rights.



Westinghouse Astronuclear Laboratory



Prepared By:

Test Engineering

Approved By:

*Robert E. Lochbaum*  
Robert E. Lochbaum,  
Manager

Test Engineering

*W. B. Henderson*  
W. B. Henderson,  
Manager

Equipment and

Facilities Engineering

Classification cancelled (changed to)  
by authority of *Doc*  
by *AF-1-C* TIC date SEP 20 1973

WANL-TNR-220

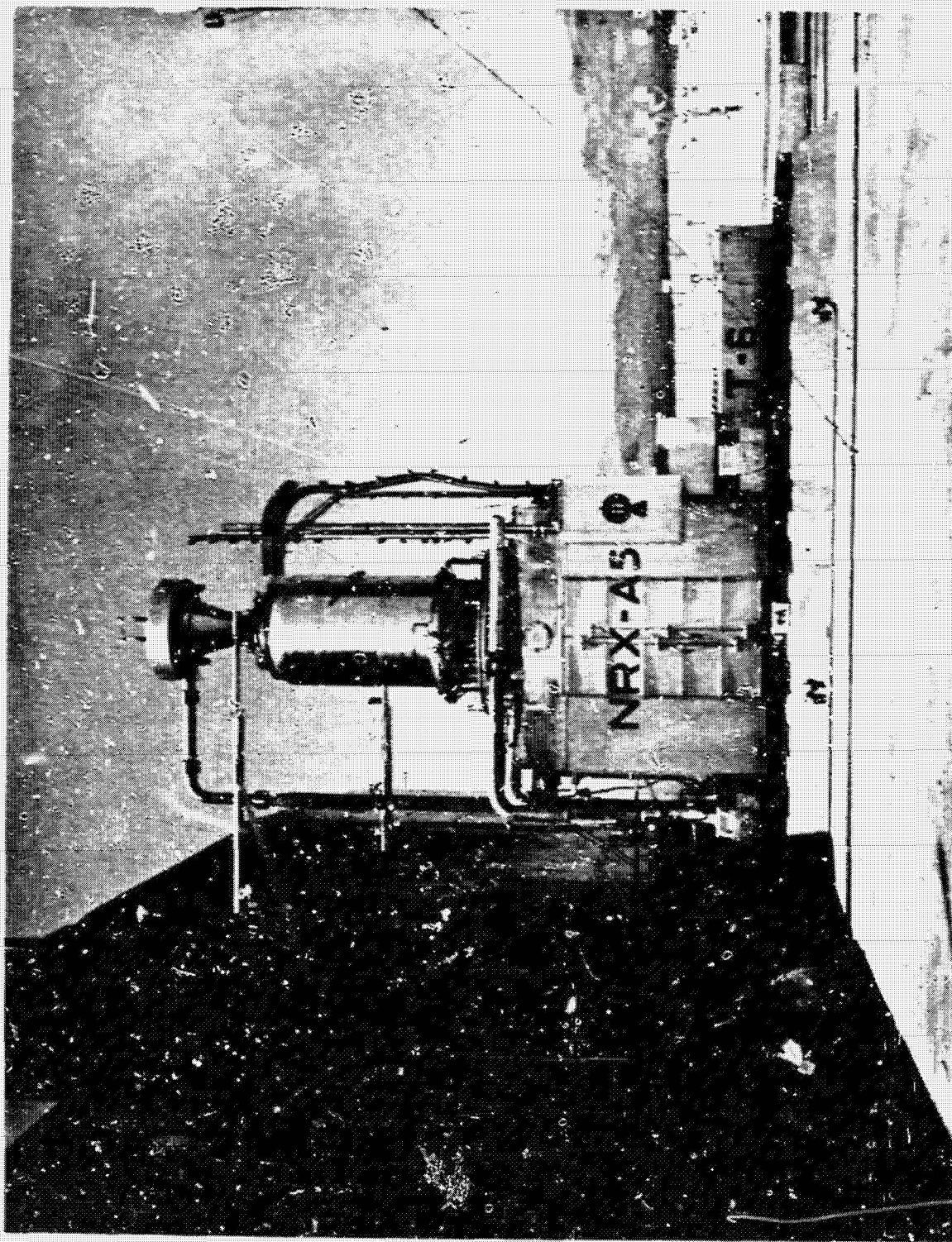
**NRX-A5 FINAL REPORT**

(Title Unclassified)

Subcontract NP-1

~~CONFIDENTIAL~~  
~~RESTRICTED DATA~~  
~~Dec 1964~~

**BLANK PAGE**



NRX-A5 Test Assembly Mated to Test Cell "A"

**BLANK PAGE**



## **ACKNOWLEDGMENT**

The material presented in this report represents contributions from members of several organizations--the Space Nuclear Propulsion Office (SNPO), Aerojet-General Corporation (AGC), NERVA Test Operations (NTO) as well as the Westinghouse Astronuclear Laboratory (WANL). At WANL, specific sections of this report were prepared by various departments--Reactor and Accessories Design, Control Systems Engineering, Thermal and Nuclear Design, and Test Engineering. Full credit is extended to these groups for their participation. The references enumerated in the bibliography of this report will provide more comprehensive information in specific areas of interest.

**BLANK PAGE**

## NRX-A5 FINAL REPORT

### TABLE OF CONTENTS

<u>Section</u>	<u>Page</u>
Frontispiece	
Acknowledgment	iii
Table of Contents	v
List of Illustrations	ix
List of Tables	xi
List of Symbols	xiii
 I. INTRODUCTION	
A. NERVA Program	1
B. Summary of Previous Reactor Tests	1
1.0 NRX-A1	2
2.0 NRX-A2	2
3.0 NRX-A3	2
4.0 NRX/EST	2
II. SUMMARY	5
III. TEST ASSEMBLY AND FACILITIES DESCRIPTION	7
A. Nuclear Subsystem	7
B. Control Systems	9
1.0 Reactor Control System	11
2.0 Feedsystem Control	11
3.0 Safety Systems	12
C. Test Facilities	13
1.0 Test Cell "A"	13
2.0 Fluid	13

<u>Section</u>	<u>Page</u>
3.0 R-MAD	16
4.0 Control Point	16
<b>IV. TEST DESCRIPTION</b>	<b>17</b>
A EP-I, Initial Criticality, Neutronics Calibration, Control Drum Worth Measurements, and Flow Tests	17
1.0 Initial Criticality	17
2.0 Neutronics Calibration	18
3.0 Control Drum Worth Measurements	18
4.0 Flow Tests	18
a. Gas Flow Tests	18
b. LH <sub>2</sub> Flow Tests	19
B. EP-II, Phase II Neutronics Calibration, Power Limiter Checkout and Valve Exercise Phase	19
1.0 Phase II Neutronic Calibration	19
2.0 Power Limiter Checkout	19
3.0 Valve Exercise Phase	19
C. EP-III, First Power Test	20
D. EP-IV, Second Power Test	21
E. EP-V, Third Full Power Test	24
<b>V. TEST RESULTS</b>	<b>27</b>
A. Performance Analysis	27
B. Reflector System, Seal System and Filler Strip Thermal Analysis	30
C. Control Drums	33
D. Core Thermal Analysis	33
E. Nuclear Analysis	37

~~CONFIDENTIAL~~



<u>Section</u>	<u>Page</u>
F. Controls System Performance Evaluation	38
1.0 Reactor Control System	39
2.0 Feedsystem Control	42
3.0 Safety Systems	42
G. Dosimetry	44
H. Post-Operative Radiochemistry	46
VI. POST-OPERATIVE EXAMINATION	51
A. Outer Reflector Sectors	51
B. Inner Reflector and Support System	51
C. Hot Buffer Filler Strips and Tiles	51
D. Nominal Filler Strips and Tiles	55
E. Filler Blocks	55
F. Support Blocks	55
G. Liner Tubes	60
H. Insulating Sleeves	60
I. Support Washers	60
J. Tie Rods	60
K. Damage to the 5F4 and 5F5 Clusters	61
L. Instrumentation	62
M. Conclusions	65
VII. FUEL ELEMENT PERFORMANCE	67
A. Breakage	67
B. Weight Loss	67
1.0 Incremental Weight Loss	71
2.0 External Surface Weight Loss	73

~~CONFIDENTIAL~~

<u>Section</u>	<u>Page</u>
C. Pinhole and Coolant Channel Exposure	76
D. Hot End Corrosion	79
E. Molybdenum Overcoating	79
VIII. BIBLIOGRAPHY	83



~~CONFIDENTIAL~~



## LIST OF ILLUSTRATIONS

FIGURE		PAGE
1	Cross Section of the Core Showing Hot Buffer and Nominal Filler Strip Design	8
2	Functional Design of the NRX-A5 Control System	10
3	Plot Plan of NRDS	14
4	NRX-A5 Flow Diagram Test Cell "A"	15
5	Reactor Performance Parameters During First Power Test (EP-III)	22
6	Reactor Operating Map For First Power Test (EP-III)	23
7	Reactor Performance Parameters During Second Power Test (EP-IV)	25
8	Reactor Operating Map For Second Power Test (EP-IV)	26
9	NRX-A5, EP-III, Decay Power	28
10	NRX-A5, Normalized Seal Chamber Pressure Profiles	32
11	NRX-A5, EP-III, Temperature Versus Radius	34
12	NRX-A5 Thermal Capsule Data Versus Core Radius	36
13	Measured Frequency Response of the Power Control Loop at 1 Kilowatt	40
14	Station 26 Temperature Profile, EP-III Ramp from 2000°R Chamber Temperature to Design Conditions	41
15	Pump Outlet Flow Rate Profile for EP-III	43
16	PCV-41 Step Responses During EP-I	45
17	Fast Neutron ( $E > 2.9$ Mev) Iso-Flux Pattern Around A Typical NRX Reactor in Test Cell "A"	47
18	Gamma Ray Iso-Dose Pattern Around a Typical NRX Reactor In Test Cell "A"	48
19	Iso-Heating Rate Contours for Aluminum Around a Typical NRX Reactor in Test Cell "A"	49
20	Filler Strip Surface Regression In Hot Buffer Area	53

~~CONFIDENTIAL~~

# LIST OF ILLUSTRATIONS

FIGURE		PAGE
21	Hot Buffer Filler Strip Corrosion	54
22	Nominal And Hot Buffer Filler Strip Design Interface	56
23	Regular Support Block	58
24	Skirtless Support Block	59
25	Severed Liner Tube, 5F5 Cluster, Station 42	63
26	Blocked Orifices, 5F5 Cluster Plate and 5F5C Fuel Element	64
27	NRX-A5 Core Exit, Showing Sooting Patterns	69
28	Fuel Element Breaks	70
29	Fuel Element Weight Loss Versus Core Radius	72
30	NRX-A5 Incremental Weight Loss	74
31	NRX-A5 Estimated Division of Fuel Element Bore and Surface Weight Loss	75
32	Comparison of Axially Sectioned Adjacent Elements	78
33	NRX-A5, $\Delta W$ Versus Radius For Batch M-32	80

~~CONFIDENTIAL~~



## LIST OF TABLES

TABLE		PAGE
1	Comparison of Steady State Test Data With Calculated Results	29
2	NRX-A5 Total Fuel Element Weight Loss	68
3	NRX-A5 Summary Data For Pinholing and Channel Exposure of Fuel Elements Examined	77

~~CONFIDENTIAL~~

**BLANK PAGE**

# LIST OF SYMBOLS

ACV	Analog Control Valve
AVV	Analog Vent Valve
Be	Beryllium
CE	Channel Exposure
cps	Counts Per Second
CRT	Control Room Time
ETS	Engine Test Stand
db	Decibel
FE	Flow Measuring Element
FBV	Fill Block Valve
GH <sub>2</sub>	Gaseous Hydrogen
GN <sub>2</sub>	Gaseous Nitrogen
gm.	Gram
He	Helium
JBV	Jog Block Valve
KW	Kilowatts
kg	Kilogram
LASL	Los Alamos Scientific Laboratory
lbs/sec	Pounds Per Second
LH <sub>2</sub>	Liquid Hydrogen
LN <sub>2</sub>	Liquid Nitrogen
mm	Millimeter
MW	Megawatts
MW-sec	Megawatt Seconds
NbC	Niobium Carbide
N <sub>d</sub>	RPM Demand

## LIST OF SYMBOLS

NRX	NERVA Reactor Experiment
NRX/EST	NERVA Reactor Experiment/Engine System Test
$N_s$	Specific Speed
$N_{sd}$	Specific Speed Demand
OBV	Open-Close Block Valve
CFV	Open-Close Fill Valve
OVV	Open-Close Vent Valve
P	Pressure
$P_{cd}$	Chamber Pressure Demand
$P_{cm}$	Chamber Pressure Measured
PCV	Pressure Control Valve
PDT	Pacific Daylight Time
psi	Pounds per Square Inch
psia	Pounds Per Square Inch, Absolute
psig	Pounds Per Square Inch, Gage
Pl	Plutonium
PT	Pressure Transmitter
$^{\circ}R$	Degrees Rankine
$^{\circ}R/sec$	Degrees Rankine Per Second
RMSF	Remote Material Storage Facility
RPM	Revolutions Per Minute
$RPM_d$	Revolutions Per Minute Demand
SV	Safety Valve
T	Temperature
$T_{cm}$	Measured Chamber Temperature
$\Delta W$	Weight Loss



## 1. INTRODUCTION

### A. NERVA PROGRAM

As the name implies, the overall objective of the NERVA (Nuclear Engine for Rocket Vehicle Applications) program is the development of a solid-core nuclear reactor-powered flight engine for space vehicles. The specific impulse advantages of such a system over chemical-powered rockets, especially in the upper stages of an interplanetary mission vehicle, have been well documented and require no discussion here. The NERVA program, which is currently in progress, is a continuation and extension of the KIWI series of tests performed by Los Alamos Scientific Laboratory. Both the KIWI and NERVA tests have utilized the test facilities at the Nuclear Rocket Development Station (NRDS) at Jackass Flats, Nevada.

Specifically, the objectives of the NERVA program are as follows:

- 1) To develop and preliminary flight rating test a nuclear engine capable of operating at full NERVA power and temperature (4200 MW and 4500°R) for 60 minutes
- 2) To evaluate the performance capabilities and to demonstrate the stable operation of the hot-bleed cycle nuclear engine system
- 3) To provide the necessary information for the design of future reactor and engine systems
- 4) To develop a simple, reliable reactor control system
- 5) To experimentally determine the extremes of the steady-state operating map of the NERVA engine
- 6) To demonstrate the multiple full power restart capability of the NERVA engine.

### B. SUMMARY OF PREVIOUS REACTOR TESTS

The reactor tests performed prior to the NRX-A5 power test series in the NERVA development program are the NRX-A1 cold flow test series, unfueled graphite core (Reference 1), the NRX-A2 power test series (Reference 2), the NRX-A3 power test series (Reference 3), and the NRX/EST engine system test series (Reference 4), the results of which are briefly summarized in this report.

Significant accomplishments of the above tests were as follows:

**1.0 NRX-A1**

- (a) Verified reactor structural integrity under rated pressure loading.
- (b) Obtained reactor performance data under ambient and cold flow conditions.

**2.0 NRX-A2**

- (a) Provided significant information for verifying the steady-state design analysis for power operation.
- (b) Provided information confirming the suitability of the reactor for operation at the steady-state levels and temperatures required of the reactor as a component of a nuclear rocket-engine system.

**3.0 NRX-A3**

- (a) Proved the capability of the reactor for continuous rated power operation for more than 15 minutes with margin for restart and operation at rated power for an additional period of 5 minutes.
- (b) Proved the capability to start up from a low-power, low-flow, steady-state operating condition and to shut down from a medium power level on liquid-hydrogen flow control only.
- (c) Provided direct performance data on the nozzle and pressure vessel
- (d) Definitely showed that the reactor is inherently stable on liquid hydrogen flow control only.

**4.0 NRX/EST**

- (a) Demonstrated the feasibility of the hot-bleed cycle nuclear engine system for transient and steady-state operation.
- (b) Demonstrated the capability of the NRX-A reactor to operate at, or near, rated conditions for a cumulative period of approximately 30 minutes. (In addition, the total equivalent run time at rated power was 54.4 minutes.)

#### 4.C NRX/EST (continued)

- (c) Demonstrated the suitability of control-system concepts and stability of the engine system for transient and steady-state conditions over a broad area of the engine operating map.
- (d) Demonstrated the multiple-restart capability of the engine system with various control modes by starting eight times to an intermediate power level and three times to rated power.
- (e) Demonstrated the capability of the engine system to accomplish bootstrap startup at a chamber-temperature ramp at or above  $100^{\circ}\text{R}/\text{sec}$ .

During the NRX-A1 tests, there was no evidence of large, low frequency vibrations (such as had occurred in the KIWI reactor series), either forced or self-excited, which would imply possible dynamic instability in the reactor assembly. The absence of these vibrations verified the adequacy of the design of the core support structure. Post-operative examination revealed few signs of the effects of the testing on the reactor components.

The NRX-A2 reactor was operated for seven (7) minutes at an average power level of 813 megawatts. The liquid hydrogen flow rate averaged  $75.6 \pm 1.5$  lbs/sec. During the seven (7) minutes the power reached  $1096 \pm 50$  megawatts for 40 seconds, which verified the ability of the reactor and nozzle to withstand the environment at full power. The specific impulse at the full-power hold was  $745 \pm 18$  seconds (corrected to vacuum), and the thrust was 55,500 pounds. During the test series, reactor stability was demonstrated with constant control drum position for propellant flow rates between 5.2 and 13.5 lbs/sec in the power range of 2.0 to 4.7 percent of full power (1120 megawatts). The fixed control drum test demonstrated the feasibility of controlling the reactor on propellant flow only. Another test was performed with flow rates between 8.3 and 13.5 lbs/sec on dewar pressure alone (no pump operating) at a constant 3.4 percent of full power.

Power testing on NRX-A3 consisted of three (3) runs. The first run (EP-IV) was terminated after 3.5 minutes at design conditions due to a spurious trip of the automatic shutdown system. During EP-V the reactor was operated for 16 minutes, 13.1 minutes of which were at



ated conditions. EP-VI was a medium power mapping and controls test. During this test, the reactor was operated over a range of power with fixed control drums, power being controlled with propellant flow rate only. This test showed definitely that the reactor is inherently stable on liquid hydrogen flow control only, which was a major step in the simplification of controls for future NERVA systems.

The NRX/EST test series coupled an NRX reactor with a "breadboard" arrangement of engine components in which the components were connected in a flight functional configuration. During this test series, the hot-bleed, bootstrap principle of nuclear rocket engine operation was utilized for the first time. Engine system stability and operability were demonstrated under a number of control modes and over a wide operating range of temperature and pressure. In accomplishing the endurance objective, the engine was operated for a total of 143.8 minutes, of which 105.6 minutes were at thrust chamber temperatures above  $1700^{\circ}\text{R}$ , 24.5 minutes were at power levels in excess of 1000 megawatts and 15.1 minutes were at thrust chamber temperature above  $4000^{\circ}\text{R}$ .

## II. SUMMARY

The NRX-A5 test series was conducted at the Test Cell "A" Facilities of the Nuclear Rocket Development Station, Jackass Flats, Nevada, between May 26, 1966, and June 23, 1966, inclusive.

The prime objective of the program was to operate at design conditions for a total accumulated time of forty (40) minutes (Reference 5). In order to accomplish this objective five (5) experimental plans (EP's) were outlined, the first two of which confirmed the readiness of the test article and test facility for full power operation.

EP-III was the first full power test. During the startup for this EP, controls and limiter checkouts were accomplished at a chamber temperature of 2000°R. On the succeeding ramp to rated conditions, an incorrect power correction factor inserted at the 2000°R hold resulted in power limiting just prior to attaining full power. The power setting was raised enough to permit full power operation.

Shortly after reaching the top of the startup ramp, oscillations were observed in power. The amplitude of the oscillations was roughly  $\pm 300$  MW. It was subsequently determined that an intermittent failure of one of the control thermocouples was the cause of the oscillation. This thermocouple was automatically rejected as an input to the control system and the run continued. After 16.1 minutes at thrust chamber temperatures above 3600°R, of which 9.3 minutes were above 3950°R, the run was terminated when the level in the LH<sub>2</sub> storage dewars reached the cut point.

Significant operations of EP-IV were (1) fixed drum startup from 30 KW to near rated conditions and (2) operation at rated conditions for approximately 14.3 minutes. The run proceeded as planned with no major anomalies noted. Rated conditions were held until the test parameter limit, a drum angle position of (145°), was reached. A normal shutdown terminated the run.

EP-V was not performed, since the pre-test determined shutdown limit, a drum angle of 145°, (Reference 6) was reached at the end of EP-IV. Although several minutes

of operating time remained on the core, the test series was terminated to preserve the core for post-operative examination.

The most significant operations and accomplishments of the Test Series were as follows:

1. The Test Assembly was operated for 29.4 minutes at, or above, chamber temperatures of  $3800^{\circ}\text{R}$  and for 22.4 minutes at, or above, chamber temperatures of  $4000^{\circ}\text{R}$  (average core exit gas temperature was at, or above,  $4000^{\circ}\text{R}$  for 24.7 minutes).\*
2. Operation of a new eight decade neutronic system was demonstrated. For EP-I and EP-IV the neutronic detectors were located on the test car under the Test Article and used as the neutronic system feedback.
3. The reactor was checked out and operated at rated conditions using a temperature control system without the neutronics power control as an inner loop.
4. The acceptability of a startup from low power to near rated conditions using programmed  $\text{LH}_2$  flow with drums in a fixed position was demonstrated.
5. The initial criticality of the reactor was performed after all poison wires were removed.

The Average Control Drum Angle Test Parameter Limit of 145 degrees was reached after a total accumulated operating time of 30.75 minutes at, or above, 1000 MW, thereby forestalling achievement of the prime objective, operation at design conditions for a total accumulated time of forty (40) minutes.

The test performance analyses and post-operative examination results are discussed in Sections V and VI, respectively, of this report.

---

\*No thermocouples existed at the core exit plane in the NRX-A5 or previous reactors. The chamber thermocouples, located approximately 17 inches downstream of the core exit plane, were the closest means of core exit gas temperature measurement. The average core exit gas temperature is approximately  $40^{\circ}\text{R}$  higher than the average gas temperature at the thermocouples, due to regenerative cooling of the nozzle.





### III. TEST ASSEMBLY AND FACILITIES DESCRIPTION

The NRX-A5 test assembly consisted of a nuclear subsystem and thrust chamber assembly mounted on a test car. The test car, with its associated piping, shielding and instrumentation was plugged into the Test Cell "A" facility at NRDS, Jackass Flats, Nevada. The frontispiece shows the NRX-A5 mounted on the test car and connected to the Test Cell.

#### A. NUCLEAR SUBSYSTEM

The heat source of the NRX-A5 was an epithermal, graphite moderated nuclear reactor having a core consisting of 1584 fueled elements, each of hexagonal cross section, approximately 0.75 inch across the flats and 52 inches long (Reference 7). The assembled core forms a cylinder approximately 35 1/2 inches in diameter and 52 inches long.

The periphery of the core was filled out to a circle by a series of filler strips. In the conventional (nominal) NRX-A5 periphery design, the filler strips were separated from the outermost fuel elements by a row of pyrolytic graphite strips. The equivalent of four sectors (108 filler strips) of the core periphery were arranged this way. The equivalent of the two remaining sectors (54 filler strips) of the core periphery incorporated the hot buffer design which places the pyrographite on the outside surface of the filler strips, causing the filler strips to operate at higher temperature and, hopefully, minimizing radial leakage through the cracks between strips. The filler strip arrangements are shown on Figure 1.

Each hot buffer filler strip was NbC coated on the outer or peripheral surface except for the last two inches of the aft end, which was completely coated. The nominal filler strips were uncoated.

Surrounding the filler strips was the lateral support and seal system which provided a positive mechanical bundling force on the core through the use of leaf springs and a pneumatic bundling force using the high inlet pressure of the propellant.

The lateral support system was supported by the inner reflector, a graphite cylinder approximately 40 inches in outside diameter. Surrounding the inner reflector was the beryllium outer reflector which had an outside diameter of 49 3/8 inches and which contained the 12 control drums.





8

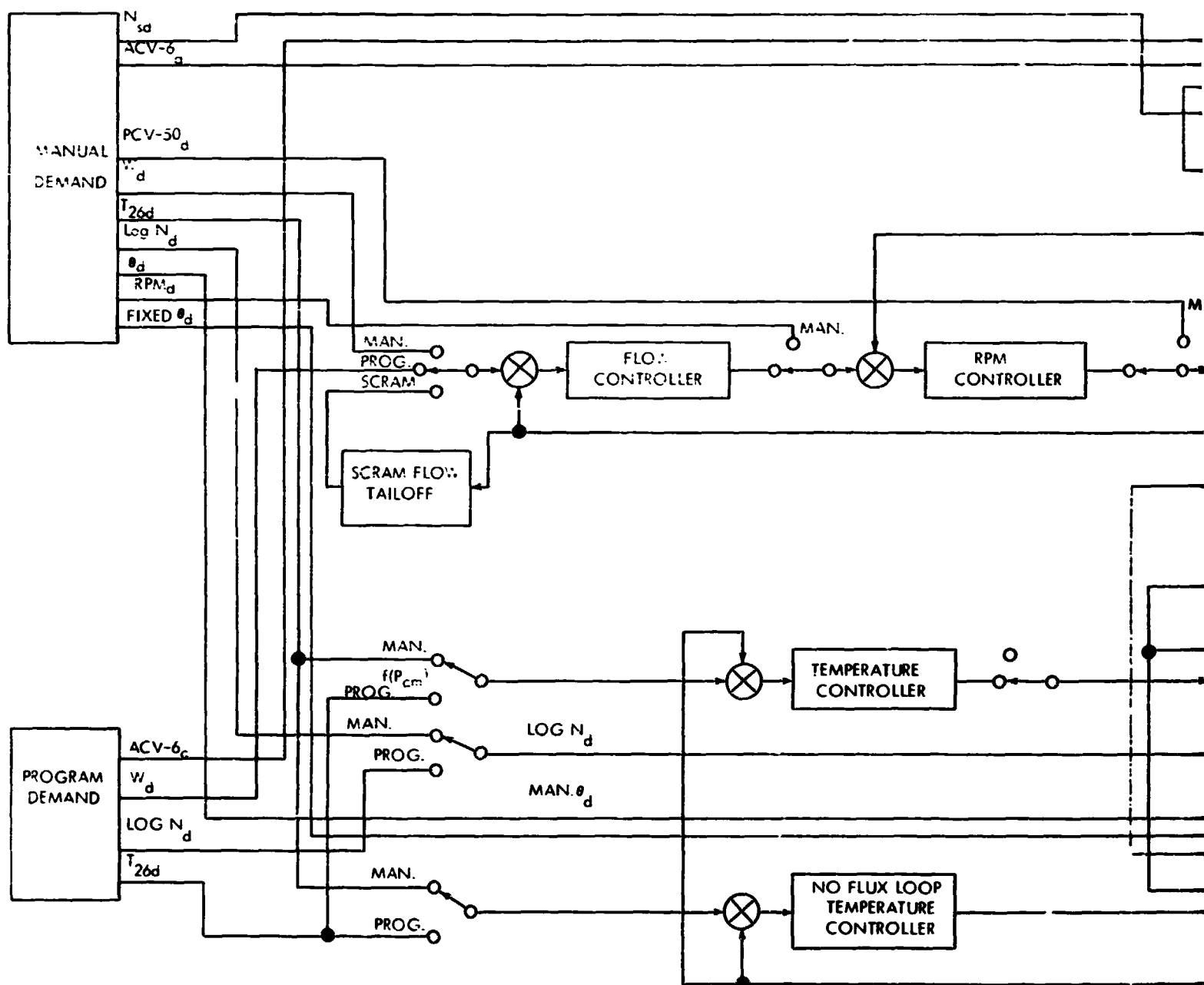
The control drums were beryllium cylinders, approximately 4 inches in diameter and 52 inches long. Boral plates, 1/8 inch thick, were located along one side of the drum covering an included angle of 120 degrees. Control of the reactor was accomplished by rotating these plates toward or away from the core.

The following are the differences between the NRX-A5 and previous reactor designs:

- 1) Elimination of the aluminum barrel surrounding the outside of the inner graphite reflector
- 2) Full length pyrographite tile on filler strips
- 3) Support blocks with modified washers
- 4) Modified fuel element ends
- 5) Control drums modified to minimize bowing
- 6) Reflector impedance ring relocated to the inlet between the inner graphite reflector and the Be reflector
- 7) Tie rod material was changed from Inconel 750 (used in the NRX/EST) to Inconel 718
- 8) Two sectors of hot buffer periphery were incorporated as an experiment
- 9) Unfueled tips brazed to the hot ends of fuel elements, included as an experiment (33 Y-12 Elements, only)
- 10) Fuel element bore coating profiles
- 11) Two fuel elements (WAFF) with molybdenum overcoated bores, included as an experiment
- 12) Six skirtless support blocks, included as an experiment.

## B. CONTROL SYSTEMS

The NRX-A5 control systems, described in detail in Reference 8, consisted of the reactor control system which provided a position signal to the reactor control drums; the feed-system controls which regulated the flow of liquid hydrogen by providing position signals to valves PCV-50 and ACV-6; and the safety system which provided protection for the reactor in the event of a malfunction. Figure 2 is a functional diagram of the NRX-A5 control system.



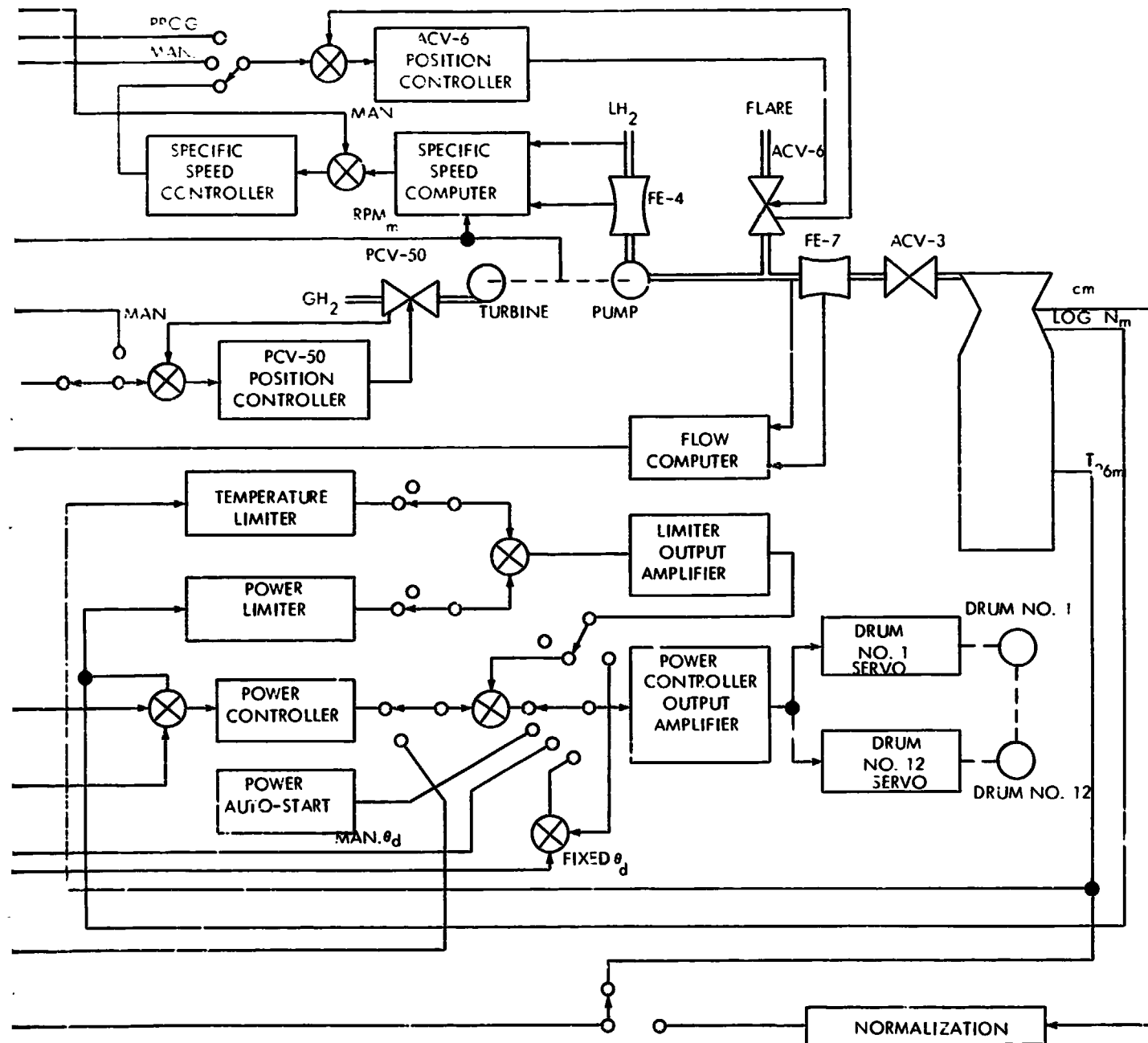


Figure 2. Functional Design of the NRX-A5 Control System

## 1.0 Reactor Control System

The reactor control system included both open and closed loop control modes and the necessary measurement for these modes. The system was made up of the following specific items: power and temperature trim control, temperature control, (this mode of control has previously been called No-flux Loop Temperature Control) drum position and fixed drum control, the automatic startup system, and the nuclear and temperature instrumentation. In the power and temperature trim control mode, the control drums were positioned to reduce the error between demanded and measured power and the power demanded was trimmed by the temperature trim controller to reduce the error between the demand and measured temperature. In the temperature control mode, the control drums were positioned to reduce the error between the demanded and measured temperature; this mode of temperature control eliminated the inner log power control loop. In drum position and fixed drum control modes, the control drums were positioned by a manual demand; the difference between the two modes was that in fixed drum control the limiters could be activated. The automatic startup system was used to bring the reactor from a subcritical shutdown condition to a pre-determined power level by programming the drum position until the pre-determined power level was reached.

The NRX-A5 nuclear instrumentation system was modified to make available the use of fixed position car mounted detectors. This system known as the Integrated Nuclear Instrumentation System (INIS) described in detail in Reference 9, consisted of four Westinghouse WX-5362 ionization chambers and associated electronics. The temperature instrumentation system provided average Station 26 temperature and average chamber temperature as feedback signals. The average Station 26 temperature was chosen for the prime control temperature, with the average chamber temperature as a backup.

## 2.0 Feedsystem Controls

The feedsystem controls were the  $\text{LH}_2$  Flow and RPM Control System which controlled PCV-50, and the Specific Speed Control System which controlled ACV-6. In addition, manual position control was provided for both PCV-50 and ACV-6.



In RPM control, PCV-50 was positioned to reduce the error between demanded and measured turbopump RPM. In  $\text{LH}_2$  flow control, an RPM demand signal was generated to reduce the error between demanded and measured pump outlet flow.

In specific speed control, ACV-6 was positioned to prevent the measured specific speed, as calculated from turbopump speed and pump inlet flow, from becoming less than the demanded specific speed.

### 3.0 Safety Systems

The safety system consisted of the scram and flow shutdown chain, the power and temperature limiters, the power and temperature limiters, the scram flow tailoff system, and the  $\text{GH}_2$  emergency cooling system.

The scram and flow shutdown chain monitored critical system parameters and provided a safety action whenever these parameters reached a pre-determined limit. The power and temperature limiters compared the measured power and Station 26 temperature with pre-set safety limits. If either the measured power or temperature exceeded the limits, the limiters moved the control drums to decrease reactivity and reduce reactor power and temperature. There were two modes of limiters available; a velocity mode for use with temperature or temperature trim control and a fixed drum mode to provide limiter protection when operating in the fixed drum mode of reactor control.

The power and temperature inhibitors were designed to deactivate the power or temperature trim controllers, if the respective error input signals to these controllers exceeded preset limits.

The scram flow tailoff system provided a programmed decrease in  $\text{LH}_2$  flow during a scram, thereby preventing a reactor overcooling following a scram and preventing the pump from entering the stall region of its operating map.

The  $\text{GH}_2$  emergency cooling systems provided control of  $\text{GH}_2$  for reactor cooling in event of a flow-shutdown.

During the NRX-A5 tests, a new period trip circuit was evaluated in a side-by-side test. The trip circuit worked on a differencing principle by comparing the change of measured log power during a pre-determined time interval with a maximum allowable change in power determined by the period trip setting. The trip circuit was designed to reduce the sensitivity of the period trip circuit to noise. In all cases tested, the period trip circuit operated as designed. No adverse noise effects were noted with this type period trip circuit.

### C. TEST FACILITIES

The NRX-A5 test series was performed at the Nuclear Rocket Development Station (NRDS), Jackass Flats, Nevada. This facility, designed and erected exclusively for the testing of nuclear rocket engines and components, is jointly sponsored by the Atomic Energy Commission (AEC) and National Aeronautics and Space Administration (NASA) through the Space Nuclear Propulsion Office (SNPO). A plot plan of the NRDS is shown in Figure 3.

Three of the major facilities at NRDS were used for the testing of the NRX-A5. These were: Test Cell "A", Reactor Maintenance and Disassembly Building (R-MAD) and the Control Point (CP).

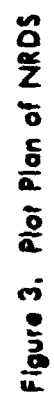
#### 1.0 Test Cell "A"

Test Cell "A" is a complex of fluid storage and piping systems, together with the necessary instrumentation and other support systems necessary to conduct tests on an NRX type test article. The NRX-A5 flow diagram of Test Cell "A" is shown on Figure 4.

#### 2.0 Fluid

Test Cell "A" has three  $\text{LH}_2$  run dewars with a total capacity of 156,000 gallons, a quantity sufficient for approximately 15 minutes of full power operation of the NRX-A5 reactor.

The  $\text{LH}_2$  propellant is pumped to the reactor by means of a turbopump driven by high pressure gaseous hydrogen stored in seven (7) high pressure storage bottles having a combined volume of 12,275 cubic feet. With an initial pressure of 3400 psig, this capacity is sufficient to support a 15 minute full power run and still maintain a reserve sufficient to



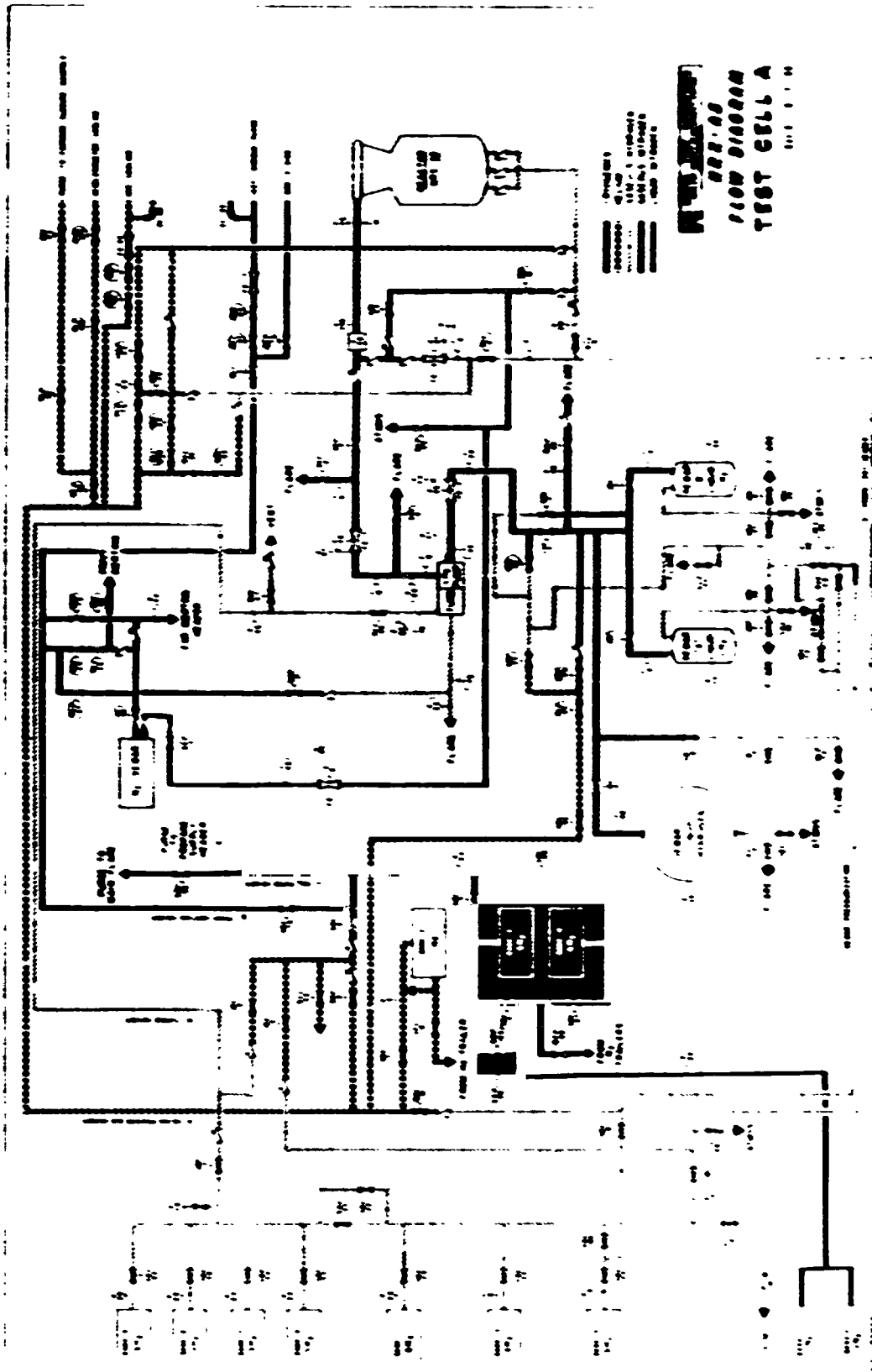


Figure 4. NRX-A5 Flow Diagram Test Cell "A"



cool the reactor in the event of a malfunction in the  $\text{LH}_2$  system. Also available for reactor cooldown and purging, are 13,000 gallons of liquid nitrogen, 3230 cubic feet of gaseous nitrogen and 1570 cubic feet of helium.

Also provided at Test Cell "A" are pneumatic and hydraulic systems for valve actuation and control drum operation, several independent electrical systems for operating the multitude of electrically driven equipment, controllers, valves, etc., and a very complete instrumentation system which is required to monitor the condition of facility equipment during a test run. In addition, the test cell has the equipment necessary to condition and transmit the hundreds of data channels monitoring the condition of the test article during the test.

### 3.0 R-MAD

Assembly of the test article on the test car and disassembly and inspection of the various components after testing is accomplished in the R-MAD Building, located some two (2) miles to the east of the test cell. This complex contains clean areas for assembly, and shielded hot cells for disassembly and inspection. Included in the hot cells are the necessary remote handling tools, manipulators and fixtures to accomplish the disassembly operation.

Transfer of the test assembly to and from the test cell is accomplished by rail, with the use of a remotely controlled locomotive and railway type test car. The mate-up of the test car to the test cell is designed to be remotely coupled and decoupled without requiring personnel on the test pad.

### 4.0 Control Point

Control of the reactor and facility equipment during a test run is handled from the CP located approximately two (2) miles south of the test cell. Contained in the CP is a control room, where a team of operators control every phase of the operation through two miles of "long lines" connecting them to the test article.

Also contained in the CP are the data recording systems which store the test information on tapes and charts for later evaluation.

#### IV. TEST DESCRIPTION

The test series consisted of five (5) experimental plans (EP's) designed to carry out the requirements of the NRX-A5 Test Specification. The five (5) EP's are individually described below.

##### A. EP-1, INITIAL CRITICALITY, NEUTRONICS CALIBRATION, CONTROL DRUM WORTH MEASUREMENTS, AND FLOW TESTS

The first set of tests of the NRX-A5 Test Series consisting of initial criticality, neutronics calibration, control drum worth measurements, and flow tests, was performed on May 26, 1966, in accordance with Reference 10.

All objectives of the EP-1 tests were successfully attained.

Virtually no problems occurred and the test was conducted as planned. Significant operations included: (1) Initial Criticality, (2) Phase I Neutronics Calibration, (3) Control Drum Worth Measurements, (4) Response Measurements on the Power Controller, (5) Ambient  $\text{CH}_2$  Flow Test, (6) Response Measurements on the PCV-41 Pressure Controller, (7) Cold  $\text{GN}_2$  Flow Test, and (8) Scram  $\text{LH}_2$  Flow Decay Tests.

##### 1.0 Initial Criticality

The initial criticality of the NRX-A5 was attained at approximately 1015 PDT with an average bank drum position of  $99.3^\circ$ . NRX-A5 was the first reactor which was taken critical with the central poison wires removed. The central poison wires had previously been removed at the R-MAD Building, see Reference 11. This technique eliminated 4 to 6 re-entries to the Test Cell, thereby shortening the approach to criticality. The method of predicting the critical drum position was obtained by plotting the inverse multiplication for three start-up channels in the Test Cell wall, versus drum position. A  $\text{Pu}^{238}\text{Be}$  source, emitting  $1.7 \times 10^7$  neutrons per second, in contact with the pressure vessel at Station 26 and reactor theta  $315^\circ$  (approximately  $180^\circ$  from the detectors) resulted in an initial net count greater than 20 cps for all channels. Shutdown measurements taken during the initial phase of operation indicated a scram time of 0.3 seconds and a shutdown margin of approximately 4.8 dollars

which compares very favorably with the measurements taken prior to initial criticality using the one drum roll out method (Reference 11).

## 2.0 Neutronics Calibration

After performing the initial criticality and scram check operations, a gold wire neutronics calibration run (10 KW for 6 minutes) was carried out. Results of this test showed both the water tank detector positions and the INIS detectors to be reading very nearly the actual reactor power.

## 3.0 Control Drum Worth Measurements

Three (3) types of drum worth measurements were performed: (1) integral worth of drum number 2, (2) relative integral worth of each of the drums, and (3) banked differential worth near the critical drum position. Evaluation of these measurements indicated the drum worth agreed with the predictions (Reference 12) and that the worths of the individual drums were essentially the same (approximately 68 cents per drum).

## 4.0 Flow Tests

### a. Gas Flow Tests

Two gas flow tests were performed. The first using gaseous hydrogen at ambient temperature and flow rates to 24 lbs/sec., provided data on system pressure drops and the performance of the PCV-41 Pressure Controller and the PCV-41 Flow Rate Controller. Step response measurements were made on the PCV-41 Pressure Controller and the PCV-41 Flow Rate Controller at 12 lbs/sec. The system pressures and pressure drops were in general as predicted (Reference 12). The performance of both the PCV-41 Pressure Controller and the PCV-41 Flow Rate Controller was satisfactory. Response measurements were also obtained on the power controller using the INIS system. The performance of the power controller was satisfactory. The second test, using gaseous nitrogen at cryogenic temperatures at a nominal flow rate of 10 lbs/sec insured that the temperature transducers were functioning properly.

b. LH<sub>2</sub> Flow Tests

Two LH<sub>2</sub> flow tests were run to check the SCRAM flow decay, the first to a flow rate of 60 lbs/sec and the second to a flow rate of 71 lbs/sec. These tests were performed with ACV-3 closed and the LH<sub>2</sub> flow by-passing the reactor to the main flare stack.

Both tests were terminated by a scram, followed by a flow shutdown from 25 lbs/sec. The performance of the scram flow decay system agreed with the analog prediction of the system performance.

B. EP-II, PHASE II NEUTRONIC CALIBRATION, POWER LIMITER CHECKOUT AND VALVE EXERCISE PHASE

Experimental Plan II of the NRX-A6 Test Series was performed on June 8, 1966, in accordance with Reference 13. Significant operations included: (1) Phase II Neutronic Calibration, (2) Power Limiter Checkout at low power, and (3) Valve exercise.

1.0 Phase II Neutronic Calibration

During this phase the Neutronic System Rams were adjusted based upon the calibration obtained during EP-I. This was followed by a set of cross-correlation measurements on the power controller at 50 KW. Results of the cross-correlation measurements are discussed in detail in Reference 14. The reactor power was then maintained at 50 KW until a power integral of approximately 15 KW-hours was obtained (for low power dosimetry irradiation).

2.0 Power Limiter Checkout

The power limiter was checked out in both the power control and fixed drum control modes, by setting the limit at 4 KW and increasing power from a 50 watt level until the limiters were observed to be limiting.

3.0 Valve Exercise Phase

All valves and systems to be used during the full power run, except those which would release gas or liquid, were exercised with the reactor at a power level of 50 watts.





### C. EP-III, FIRST POWER TEST

Following the completion of EP-II, Experimental Plan III was also accomplished on June 8, 1966, in accordance with Reference 15. The major objective of EP III was to operate the test article at rated conditions for the maximum duration compatible with the liquid hydrogen storage capabilities of Test Cell "A".

Significant operations included:

- 1) Operation at or above 1000 MW for 16.1 minutes
- 2) Checkout of the power and temperature limiters
- 3) Cross-correlation measurements on the RPM loop at rated conditions
- 4) Checkout and operation with the no-flux Temperature Controller

Following an autostart to a power level of one megawatt, the full power test was initiated with power, Station 26 temperature, and  $\text{LH}_2$  flow rate programmed. The chamber temperature was ramped to  $2000^\circ\text{R}$  at  $50^\circ\text{R}/\text{sec}$  at which point the temperature limiter was checked out. Reactor control was then switched to no-flux temperature control and a response measurement performed. Following a thermal calibration, the chamber temperature was ramped up to design power at  $50^\circ\text{R}/\text{sec}$ . The power limiter was activated at 80 percent power and began to limit just prior to attaining full power conditions, necessitating raising the setting enough to operate at full power conditions. There were moderately severe oscillations in power, shortly after reaching full power. These lasted for 25 seconds and were attributed to a shorted T-26 thermocouple. This problem is discussed further in Subsection V.F.1 of this report.

After reaching design point conditions, the power and temperature limiter and their interactions were checked out both in no-flux loop temperature control and fixed drum control. This was followed by cross-correlation measurement on the RPM loop. The reactor was then held at design point for the duration of the test cell liquid hydrogen capabilities. The full power hold was terminated at the  $\text{LH}_2$  cut point of 5,800 pounds in Dewar C following the isolation of Dewars A and B at 3,500 pounds. The lower limits on gaseous hydrogen supplies were not reached. Chamber temperature was then ramped down to  $2500^\circ\text{R}$  at which point the reactor was scrammed. This was followed by a flow shutdown at  $1500^\circ\text{R}$  chamber temperature.

The total time at or above 1000 MW was 16.1 minutes and the total integrated power for the first full power test was  $1.1 \times 10^6$  MW-sec. Figures 5 and 6 show reactor performance parameters and operating map, respectively for EP-III.

The post-test criticality measurement was made on June 8, 1966. The drum bank average critical position, with the reactor at nominal ambient conditions, varied between  $102.6^\circ$  and  $103.4^\circ$ , depending on the power level. The drum bank critical position prior to EP-III was  $98.8^\circ$  as determined during the scram check phase of EP-II. This gave an apparent drum position change, from pre-test to post-test, of approximately  $4^\circ$  and indicates that the fuel element corrosion was within predications (Reference 7). It was also noted that preliminary evaluation of the effluent cloud samples shows that the  $\text{Mo}^{99}$  concentration (used as a measure of corrosion) was only 1/20th of the concentration found in the effluent cloud from EP-IVA of NRX/EST.

#### D. EP-IV, SECOND POWER TEST

The fourth and last set of tests of the NRX-A5 Test Series was performed on June 23, 1966, in accordance with Reference 16. The major objective of this experimental plan was to operate the test article at rated conditions for maximum duration of the test cell liquid hydrogen storage capabilities.

Significant operations included:

- 1) Fixed drum startup from 30 KW to near rated conditions
- 2) Operation of the reactor at or above 1000 MW for approximately 14.7 minutes

In preparation for the fixed drum startup (no drum movement), a power level of 30 KW was established; the drums were rotated in two (2) degrees from the cold critical position (making the reactor subcritical); and the  $\text{LH}_2$  flow rate was ramped to 10 lb/sec and held (reactor brought to criticality on  $\text{LH}_2$  alone). When the power had increased to 20 MW, the  $\text{LH}_2$  flow rate was ramped to rated in a flow manner to give a nominal  $50^\circ\text{R/sec}$  chamber temperature ramp. Control was then switched to No-flux Temperature Loop and chamber temperature and power increased to rated conditions. While at rated conditions several small correc-

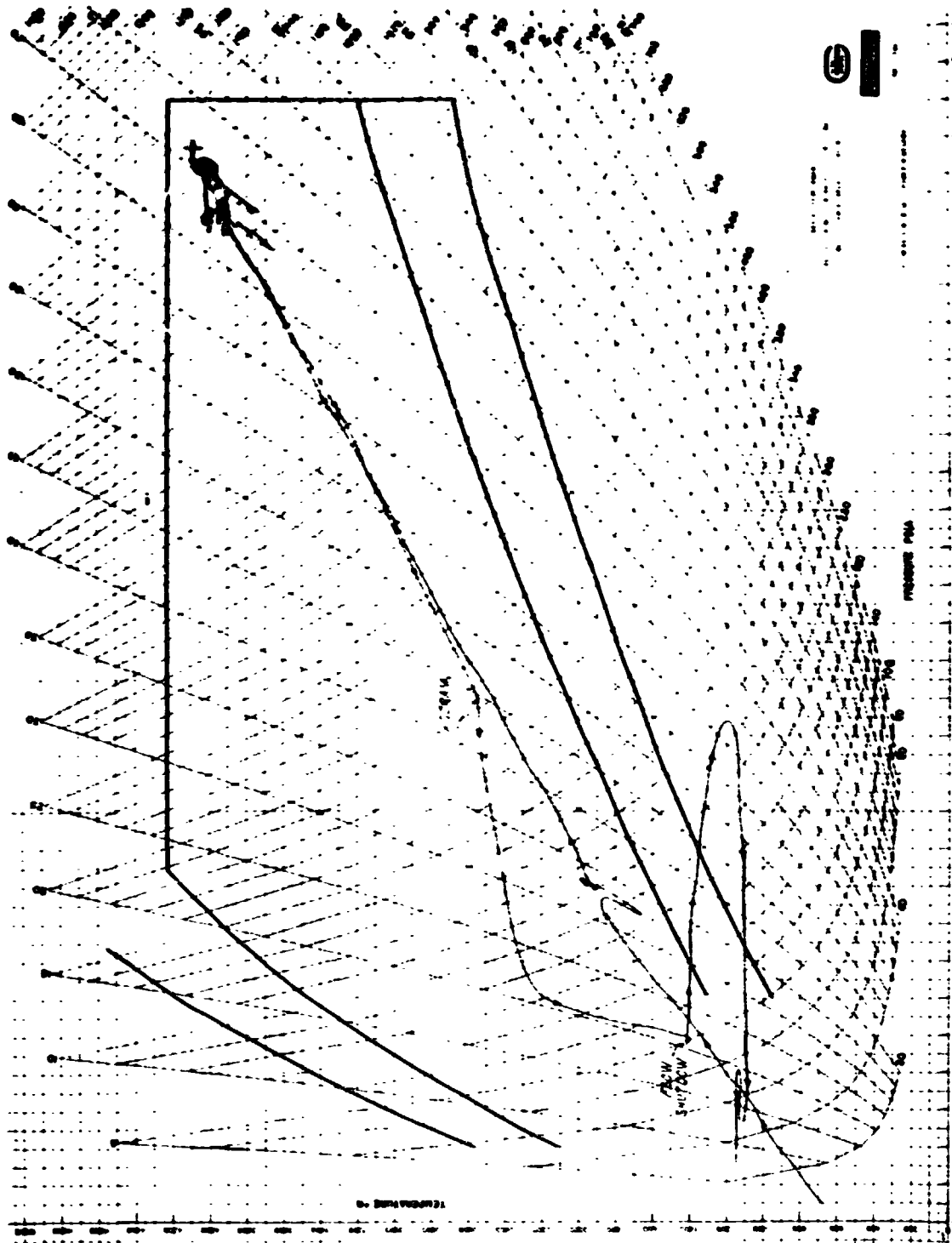
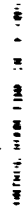


Figure 5. Reactor Performance Parameters During First Power Test (EP-III)



**Figure 6. Reactor Operating Map For First Power Test (EP-III)**



tions were made to the Station 26 temperature demand in order to maintain a chamber temperature of approximately  $4090^{\circ}\text{R}$ . Rated conditions were held until the test parameter limit a drum position of  $145^{\circ}\text{R}$  was reached. A normal shutdown was then carried out with a scram initiated at  $2500^{\circ}\text{R } T_c$  and a flow shutdown at  $1500^{\circ}\text{R } T_c$ . All facility and control systems performed as expected and no major anomalies were noted.

The post-test critical measurements for EP-IV were performed on June 27, 1966. The critical drum position at near ambient conditions (at a power level of 50 KW) was found to be  $137.9^{\circ}$  (pre-test drum position was  $102.6^{\circ}$  as determined during 50 watt scram checks). Measurements taken during the post-test criticality test were used to determine that the shutdown margin at the  $138^{\circ}$  drum position was approximately 57.9 which compares favorably with the test predictions (Reference 12).

All objectives, except the major objective, were successfully carried out. The Average Control Drum Angle Test Parameter Limit of  $145^{\circ}$  was reached after 14.7 minutes of reactor operation at or above 1000 MW, precluding achievement of the major objective. Enough liquid hydrogen remained for approximately two minutes of full power testing. Figures 7 and 8 show reactor performance parameters and operating map, respectively, for EP-IV.

#### E. EP-V, THIRD FULL POWER TEST

EP-V (Reference 17) was not performed because the pre-test determined shutdown limit, an average control drum angle of  $145^{\circ}$ , was reached at the end of EP-IV.

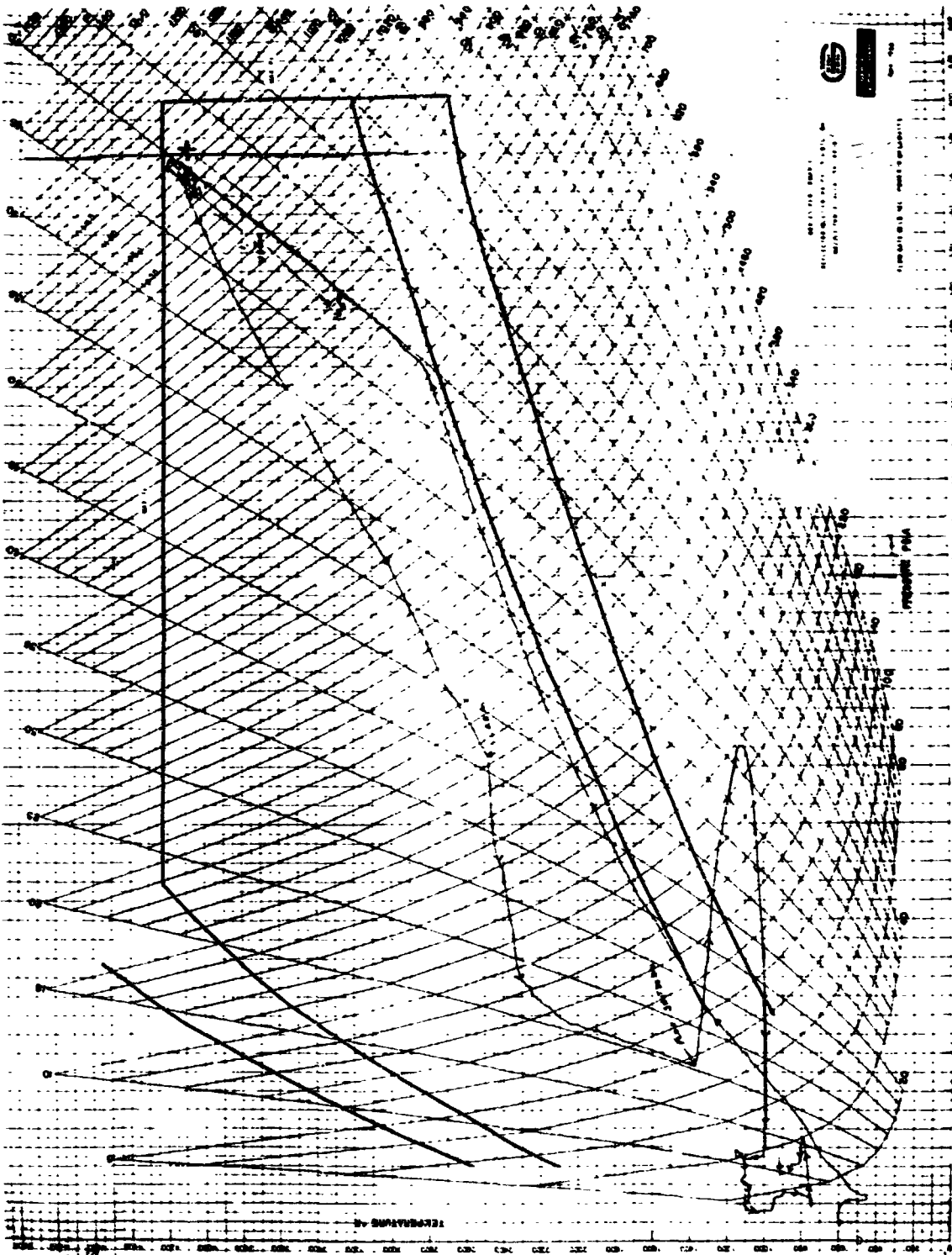


Figure 7. Reactor Performance Parameters During Second Power Test (EP-IV)

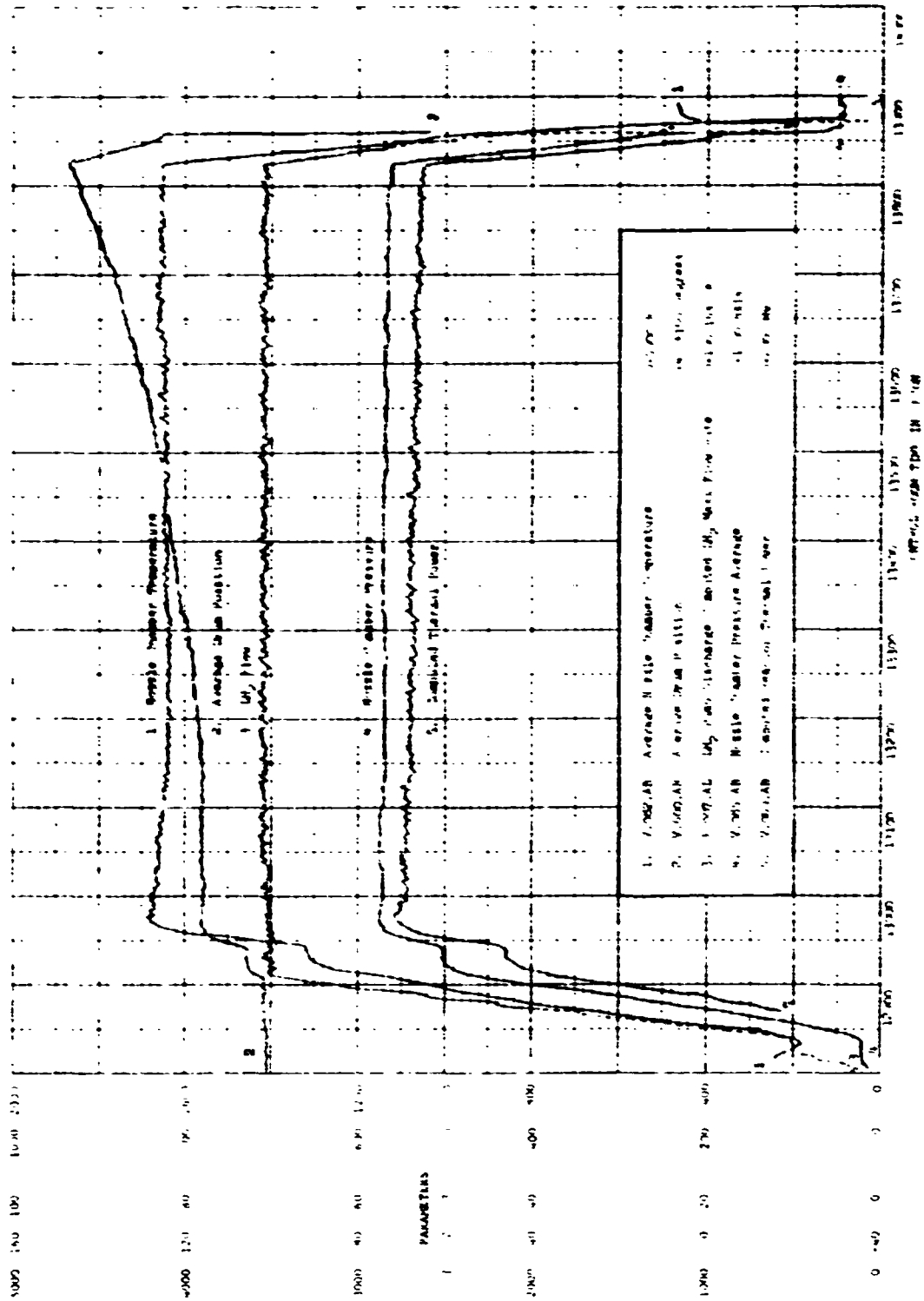


Figure 8. Reactor Operating Map for Second Power Test (EP-IV)

## V. TEST RESULTS

### A. PERFORMANCE ANALYSIS

Two full power endurance tests were performed during the NRX-A5 test series. The second test featured a fixed control drum startup over the greatest power range for this mode of startup (30 KW to near full power) to date in the NRX testing program. The startup was extremely smooth with a peak rate of change of chamber temperature of  $55^{\circ}\text{R}/\text{sec}$  and a minimum reactor period of 1.8 seconds. The accumulated run time for both endurance tests was 30.1 minutes above  $3700^{\circ}\text{R}$  nozzle chamber temperature and 26.5 minutes above  $3900^{\circ}\text{R}$  nozzle chamber temperature.

Best estimated chamber temperature, flow rate, and thermal power were computed for 10 steady state points. Steady state comparisons between test data and TNT (Thermal and Nuclear Transients Program) calculations were made for four of these points; two points each for EP's III and IV. The comparison between the measured and calculated performance parameters for the four steady state points is presented on Table 1. In addition, transient comparisons were made for both startups and the EP-IV shutdown. The comparisons between test data and calculations are reasonably good for all performance parameters. The input parameters for the EP-IV startup calculation were control drum position and flow rate. The calculated power based on these inputs is in good agreement up to 400 MW; at higher power the computed power is about 10 percent low.

The nuclear decay power was computed from test data obtained during the cooldown following the first power test, EP-III. Figure 9 shows the calculated and predicted decay power. The comparison extends from 0.5 to 4.5 hours after scram and covers a power range from 2200 to 200 KW. The experimental decay power compares satisfactorily with the decay power predicted by Revision 1 of the S-4 (Fission Product Energy Release) code.

Data obtained during the neutronic calibration test of EP-II was used to determine the relationship between rate of core temperature change and power without coolant flow. This analysis indicated that a detailed multi-node model of the core and reactor is required to adequately simulate this relationship. The computed temperatures showed good agreement



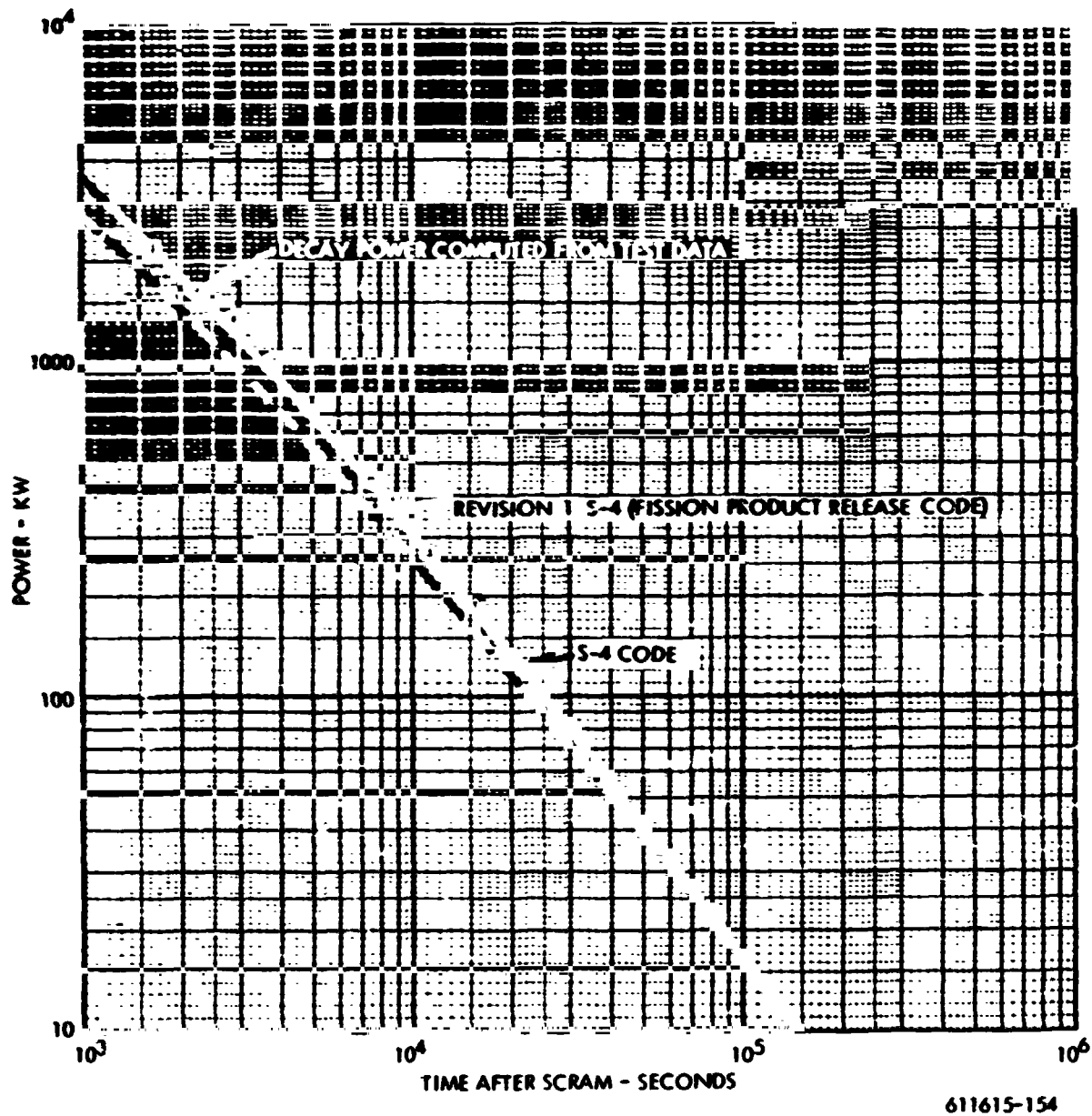


Figure 9. NRX-A5, EP-III, Decay Power

Table 1

## Comparison of Steady State Test Data with Calculated Results

EXPERIMENTAL PLAN CONTROL ROOM TIME	III 25247.5		IV 12940.0		IV 13002.5	
	Measured	TNT	Measured	TNT	Measured	TNT
Reactor Power - MW	228.8		1118.5		847.0	
Inlet Flow - LB/SEC	33.3		71.5		71.1	
Nozzle Torus:						
T - °R	45.0	44.7	52.0	52.5	52.4	52.5
P - psia	258.2	260.6	878.0	884.8	875.4	883.0
Reflector Inlet:						
T - °R	76.2	65.8	153.7	148.2	153.2	149.2
P - psia	231.2	229.8	735.3	739.6	729.4	738.0
Reflector Outlet:						
P - psia	220.0	221.5	699.0	706.1	697.3	704.6
Shield Dome Plenum:						
T - °R	103.7	102.0	221.4	233.6	171.3	235.2
Core Inlet:						
T - °R	116.4	108.1	241.7	244.2	191.1	245.8
P - psia	219.6	218.4	690.4	695.3	601.4	693.9
Core Exit:						
T - °R	1922.2	1909.8	4088.2	4080.6	3239.8	4107.7
P - psia	171.3	179.2	570.3	574.4	498.4	573.1
Tie Rod Exit:						
T - °R	442.5	463.3	664.9	675.5	502.7	682.8
Unfueled Element	Station 8 713.9	796.0	1935.1	1894.0	1535.6	1906.0
Temperatures °R	Station 20 1277.3	1230.0	3220.8	3095.0	2653.5	3115.0
	Station 26 1581.9	1470.0	3749.1	3684.0	3064.4	3708.0
	Station 32 1816.4	1690.0	4045.4	4152.0	3591.9	4178.0
Pressure Drops:						
Reactor	52.4	50.6	167.4	165.2	145.4	164.9
Core	38.4	39.2	118.3	120.9	102.6	120.8
Reflector	8.0	8.4	32.1	33.4	27.3	33.4
Shield & SP	3.4	3.0	12.0	10.8	8.9	10.8
Nozzle	26.4	30.8	140.0	145.2	114.9	145.0

~~CONFIDENTIAL~~

with test data for a power 10 percent above measured nuclear power. During EP-III the measured nuclear power (Linear Channel No. 1) was 10 percent lower than the best estimated thermal power. Therefore, on a qualitative basis, thermal power calibration is feasible for calibrating the nuclear power measuring instruments.

A comparison of heat generation in the peripheral reactor components (reflector system, pressure vessel, shield, core support plate) was made for NRX-A5 and NRX/EST, primarily to determine the effect of the external shield on the NRX/EST. Thermal data were analyzed in several ways but since the uncertainties were of the same order of magnitude as the calculated shield effect, it was concluded that an accurate evaluation of the increased heating resulting from the external shield could not be made from the available temperature data.

A comparison of average Station 26 temperature with average chamber temperature for both NRX/EST and NRX-A5 indicates that either measurement could be used as the primary control temperature.

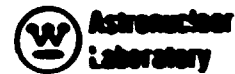
#### B. REFLECTOR SYSTEM, SEAL SYSTEM, AND FILLER STRIPS THERMAL ANALYSIS

The average measured reflector pressure drop during the EP-III NRX-A5 full power hold was 34 psi ( $2\sigma$  variance  $\pm 2.2$  psi) as compared to the calculated value of 35 psi, and during the EP-IV full power hold, it was 31 psi ( $2\sigma$  variance  $\pm 3.6$  psi) as compared to the calculated value of 34 psi. The average reflector system pressure drop at full power for previous reactors was 41 psi in NRX-A2, 41 psi in NRX-A3, and 43 psi in NRX/EST. The reduction in the reflector pressure drop in NRX-A5 was primarily due to the redesign in the reflector cooling channels, namely, the addition of a longitudinal slot in the control drum cylinder and the enlargement of the cooling hole size in the inner reflector barrel.

The measured sector and drum material temperatures at full power conditions compared very well with post-test calculations. Continued temperature increases of the beryllium and the graphite during the full power holds were also observed in NRX-A5 as in NRX-A2, NRX-A3, and NRX/EST. The average rates of temperature rise at Station 32 for these

~~CONFIDENTIAL~~

~~CONFIDENTIAL~~



reactors are approximately as follows: for beryllium,  $1.2^{\circ}\text{R}/\text{min}$ , and for the graphite barrel,  $7.2^{\circ}\text{R}/\text{min}$  at  $R = 19.2$  inches, and  $18.5^{\circ}\text{R}/\text{min}$  at  $R = 18.2$  inches.

At the start of the first full power endurance test the seal chamber coolant axial pressure distribution was the same as predicted, but as the test continued, the pressure at the core mid-band region decreased with test time, as shown on Figure 10, which compares the performance of the lateral support seal system in NRX-A5 and NRX/EST. The degradation of the seal chamber pressure was caused by core periphery corrosion which perturbed the coolant flow in the seal chambers.

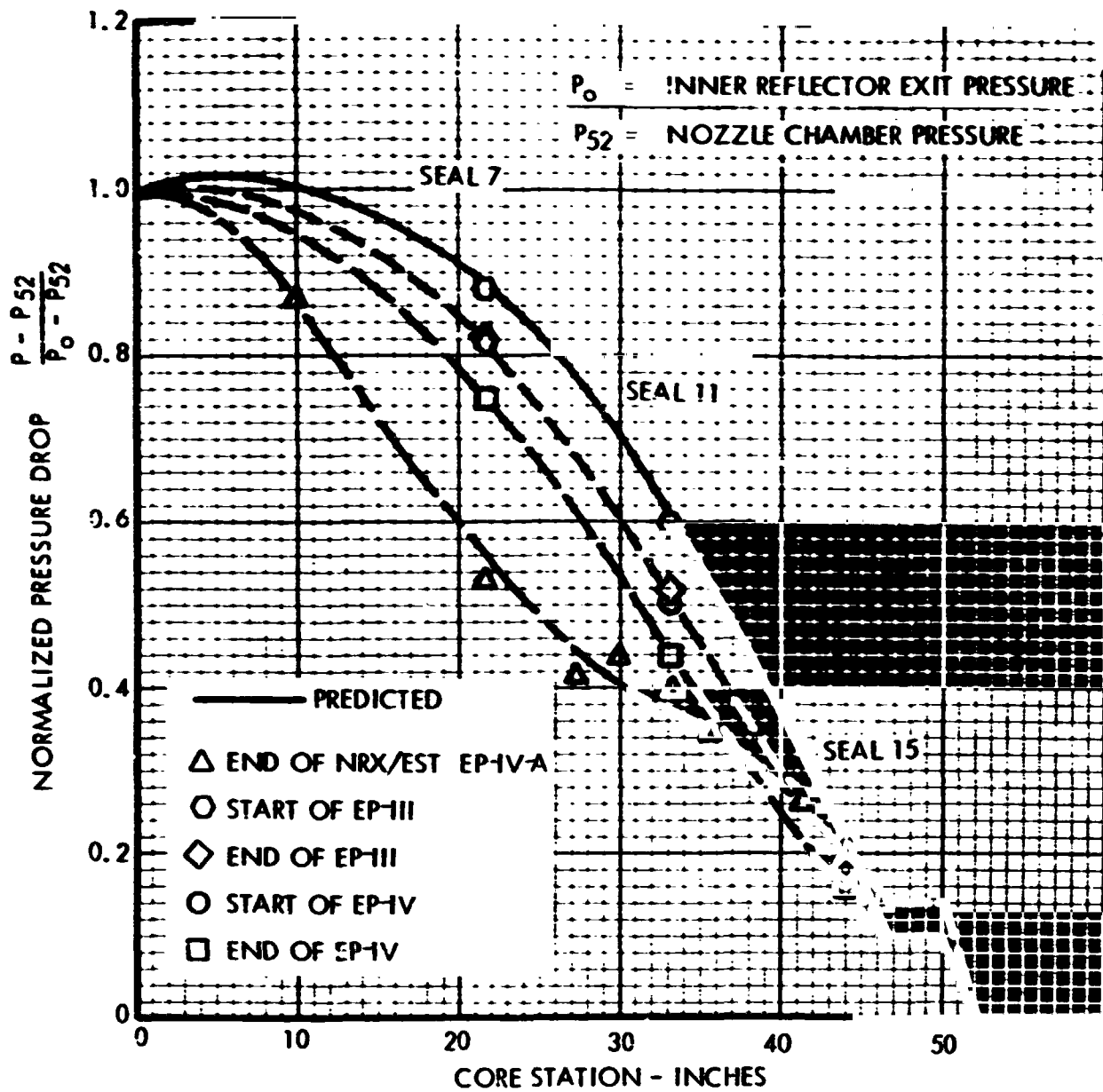
Transient thermal analysis of the hot buffer filler strips was performed in some detail because 39 of the 54 strips in the hot buffer region were found to be broken in one or more places during the post-operative examination. However, all the strips in the nominal region remained intact. It was hypothesized that bridging of the hot buffer filler strips occurred during reactor shutdown. The temperature differential between bridged filler strips resulted in severe tensile stresses in some cases. The temperature differential was due to the different strip thicknesses. An analysis of the EP-IV shutdown transient, performed for a 30 degree sector of the hot buffer filler strips resulted in a maximum calculated temperature difference of  $600^{\circ}\text{P}$  between the sector average and the coldest strip at Station 38 inches.

Steady-state maximum temperatures in filler strips were measured using thermal capsule placements in five hot buffer filler strips and one nominal filler strip. The indicated thermal capsule temperatures in the hot buffer filler strips were generally in agreement with predicted values (Reference 7) except at the hot end where the measured temperatures were lower than predicted, i.e., about  $1000^{\circ}\text{R}$  lower than the  $4400^{\circ}\text{R}$  value predicted at Station 50 inches. Thermal capsule temperatures measured in the nominal filler strip were within the range of predicted values.

Aside from the hot buffer filler strips, the reflector and lateral support system performed satisfactorily during the NRX-A5 power tests. All reactors from NRX-A3 through NRX-A5 performed consistently and all predictions and post-test calculations agreed favorably with observations.

~~CONFIDENTIAL~~

CONFIDENTIAL



611615-180

Figure 10. NRX-A5, Normalized Seal Chamber Pressure Profiles

CONFIDENTIAL

~~CONFIDENTIAL~~



With the exception of the hot buffer filler strip region in NRX-A5, the models and the analytical procedures for the reflector system of the NRX reactors are satisfactory and can provide design evaluation and predictions with a high degree of accuracy. For the filler strip region, a more detailed analytical model is required.

#### C. CONTROL DRUMS

The measured maximum temperature differences across the diameter of the control drum at core Stations 8 and 32 were less than  $15^{\circ}\text{R}$  during the EP-III and EP-IV startups. This temperature difference is very small compared to the maximum value of  $220^{\circ}\text{R}$  observed in NRX-A1 (cold flow tests),  $120^{\circ}\text{R}$  in NRX-A3, and  $80^{\circ}\text{R}$  in NRX-EST. This significant reduction in temperature difference was due to the cooling channel (a slot of 110 degree arc length and 0.116 inch depth) added in the control drum cylinder opposite the vane. The coolant flow in the slot tends to equalize the chilldown effect on both sides of the cylinder so that the resultant thermal bow was reduced. Control drum rubbing did not occur during the NRX-A5 startups.

#### D. CORE THERMAL ANALYSIS

The NRX-A5 overall performance agreed reasonably well with pre-test and post-test predictions using analytical models similar to those used for previous reactor analyses.

Temperature distributions within the core were obtained from the continuously recording thermocouples located in the unfueled elements at Stations 8, 20, 26 and 32 and from thermal capsules which were also located in the unfueled elements and indicated maximum temperatures achieved during the test. There were also six thermocouples located in a 0.024 inch diameter hole drilled into the inlet end face of three fueled elements, 1A1G, 5J9T and 6J4H. Each of these elements had one thermocouple at core Station 0.5 inch and at core Station 1.0 inch. Thirty-two of the thermocouple locations were preselected to provide data for a post-test statistical analysis. The temperature distributions during steady-state operation were essentially flat with minor variations caused by local differences in core inlet temperature and a major variation caused by corrosion and drum movement near the end of the EP-IV. Figure 11 indicates the flat temperature profile at the start of the EP-III high power hold.

~~CONFIDENTIAL~~

**CONFIDENTIAL**

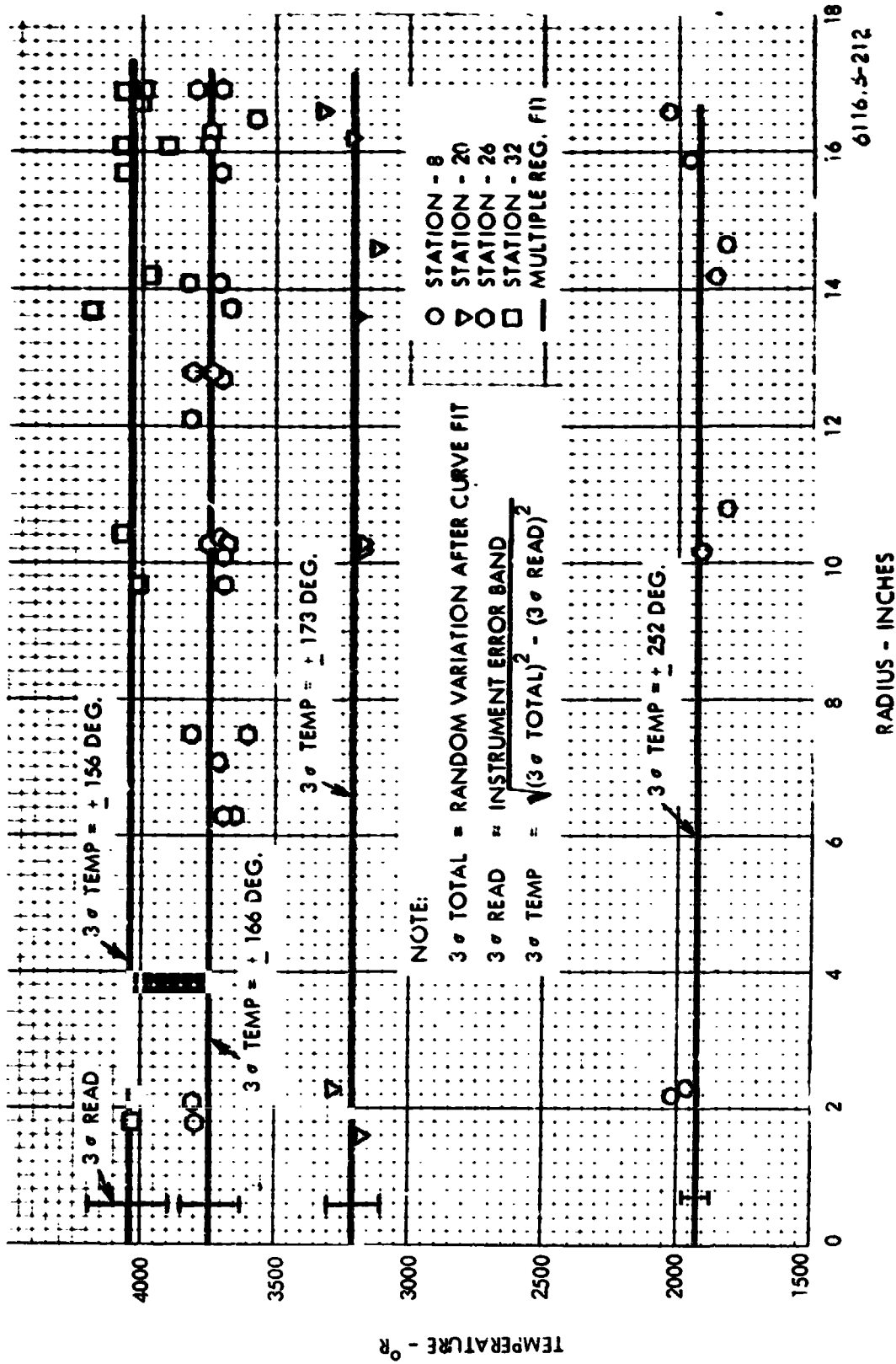


Figure II. NRX-A5, EP-III, Temperature Versus Radius

**CONFIDENTIAL**

~~CONFIDENTIAL~~



Thermocouples in the core central region experienced a sharp decrease in temperature at various times during EP-IV under otherwise steady-state conditions. It is believed that this behavior was due to severe local corrosion of the fuel elements.

The maximum temperature in the core central region, measured with a thermal capsule at Station 44 in an unfueled element, was  $4700^{\circ}\text{R} \pm 100$  as shown on Figure 12. This temperature probably occurred at the start of EP-III with the control drums at 109 degrees. The maximum temperature measured at the core periphery was  $4840^{\circ}\text{R}$  which probably occurred at the end of the EP-IV with the control drums at 145 degrees. The average calculated fuel element exit gas temperatures that corresponded to these maximum sensor temperatures were  $4277^{\circ}\text{R}$  and  $4275^{\circ}\text{R}$ , respectively.

Analysis of variance on the core thermocouples indicated a slight radial and circumferential temperature variation throughout most of the full power life, but that a strong radial effect did not appear until the end of EP-IV. During full power operation with the control drum position varying from 109 to 145 degrees, no azimuthal temperature variation related to power scalloping due to control drum rotation was detected. At the low power (229 MW) hold in EP-III with control drums at 97 degrees, the station 26 thermocouples indicated a slight azimuthal temperature variation, which could have been related to the power scalloping.

Measurements of core pressure drop were from 5% to 8% lower than post-test calculations at the full power holds. Part of this difference is attributable to a change in flow impedance caused by significant bore corrosion and part must be attributed to lower friction factors than predicted.

The tie rod material temperatures at the core exit plane were measured in seven clusters and were nominally in agreement with calculated values at full power. At low power, the calculated temperatures were about  $60^{\circ}\text{R}$  cooler than measured. The latest thermal conductivity data on pyrographite sleeves was used for these calculations.

Cracks at the corners of the peripheral fuel elements were observed in the NRX-A5 and previous reactors. One possible contributing cause of these cracks could have been temperature variations within elements and between elements during transients. A transient thermal

~~CONFIDENTIAL~~



CONFIDENTIAL

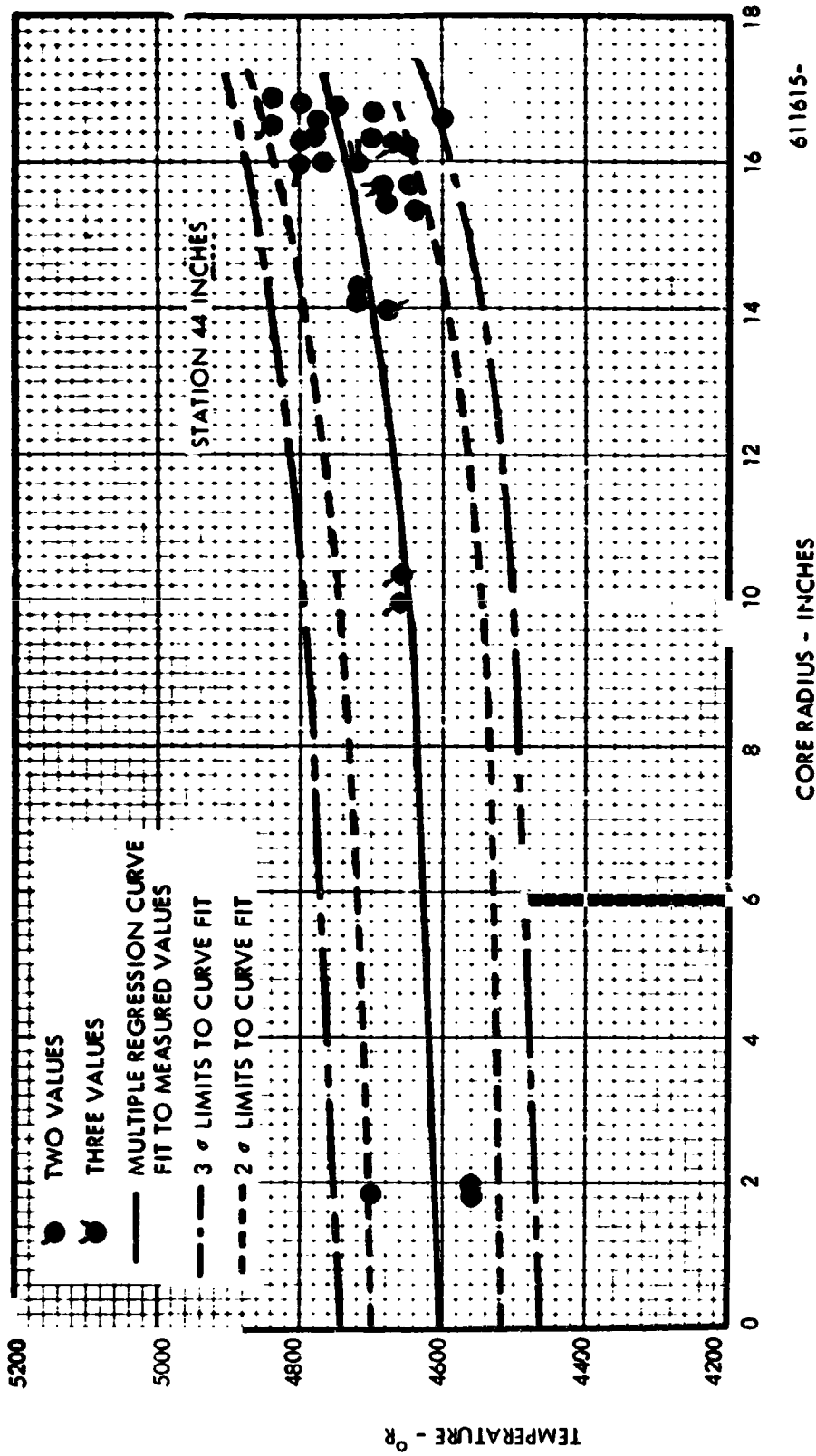


Figure 12. NRX-A5 Thermal Capsule Data Versus Core Radius

CONFIDENTIAL

**CONFIDENTIAL**



analysis on a portion of the J9 fuel cluster was performed. Stress analyses indicated that the calculated temperature variations alone were insufficient to have caused failure of the elements unless the cross section was considerably weakened by corrosion. The rothing of the outer-most corners of the peripheral fuel elements in the nominal (cold) filler strip sectors appeared to have been caused by the radial inflow of lateral support coolant.

#### E. NUCLEAR ANALYSIS

Analysis of the NRX-A5 and NRX/EST data indicates that detector placement has proved to be of high importance in deriving quantitative sub-criticality by the inverse multiplication method. Although the estimated shutdown is relatively insensitive to axial displacement of the detector from the source plane for the source-detector-reactor geometries tested, it is a function of the radial distance of the detector from the reactor vessel surface. A "close-in" detector at a four-inch distance can be expected to give a conservative estimate of shutdown, while extrapolations from a "far-out" detector, at a 36 inch distance, should be suspected as nonconservative.

An understanding of the inherent reactivity of the NRX-A5 reactor was demonstrated by the relatively close prediction of initial criticality. The actual critical drum position of 99.3 degrees compared well with the final prediction of 95.0 degrees and reasonably well with the  $93 \pm 7$  degree angle originally sought at the time of reactivity shimming during assembly.

It has been shown that the inverse multiplication technique, if calibrated by rotating one drum to  $180^\circ$ , may be used to quantitatively estimate shutdown in dollars. In the deeply shutdown condition (about \$10) conservatism is good and as the poison-wire-free condition is approached, precision becomes very good.

The analysis of drum worth data (1) confirmed the uniformity of the individual drum worths, (2) showed that single drum insertion and single drum withdrawal techniques are essentially equivalent, and (3) indicated that the NRX-A5 control drum span was \$8.2 compared with the predicted  $\$8.5 \pm 0.3$ . The power control technique used for uniformity of measurements in this test series is evaluated as excellent and is recommended for further use.

**CONFIDENTIAL**

The low power, core Station 8, temperature coefficient of reactivity, inferred from the test data as  $-0.182 \text{ } \beta / ^\circ\text{R}$ , is in excellent agreement with the NRX/EST value of  $-0.19 \text{ } \beta / ^\circ\text{R}$ . The power range over which this coefficient is clearly applicable, is approximately 50 to 100 KW. Use of the analytical core coefficient,  $-0.11 \text{ } \beta / ^\circ\text{R}$ , should be continued at conditions of very low power (100 watts, for example) and where core temperatures are fairly uniform.

The beryllium reflector temperature coefficient of reactivity has been found to be in the range of  $+0.069$  to  $+0.092 \text{ } \beta / ^\circ\text{R}$  near ambient temperature. Agreement with the calculated coefficient,  $+0.0943 \text{ } \beta / ^\circ\text{R}$ , is reasonably good. Thus, the calculated reflector coefficient can remain in use for correction of near-ambient reactor conditions.

The total reactivity loss in the NRX-A5 test series was  $2.36$ , based on the change in ambient critical positions. The variation of the loss with time was again found to be exponential, taking the form:

$$\Delta \rho (\beta) = 5.7 (\exp (t/8.23) - 1.0)$$

This loss function has been supported by statistical analysis.

The  $50\beta$  discrepancy in EP-IV, between reactivity loss during operation and that inferred from the pretest and post-test criticals as indicated by early analysis, has been explained essentially by hydrogen accumulation in the corroded areas and hydrogen diffusion into the natural pores of the fuel in the early stages of the test.

The NRX-A5 reactivity swings to full power are well represented by the NRX/EST empirical reactivity feedback model. The one sigma uncertainty in the model has been found to be  $7.25\beta$ , with a 98 percent confidence range from  $5.22\beta$  to  $11.63\beta$ .

More complete information on NRX-A5 performance analysis, thermal analysis, nuclear analysis and associated analysis is given in Reference 18.

#### F. CONTROL SYSTEMS PERFORMANCE EVALUATION

All NRX-A5 control systems operated satisfactorily and as predicted. The only anomalies which occurred were caused by component malfunction.

~~CONFIDENTIAL~~

## 1.0 Reactor Control System

During EP-I, frequency response measurements were made of the power control loop. The test data from these response measurements show good agreement with the predicted performance, see Figure 13. The temperature trim control mode was used, only during EP-III, to ramp the chamber temperature to 2000°R. The temperature trim controller performed satisfactorily and as expected.

The development of the temperature control mode, of the reactor control system, was completed with the NRX-A5 tests. This controller had not been previously used on a NERVA reactor at design conditions. The temperature control mode was introduced during the 2000°R chamber temperature hold, which insured the stability of the temperature control loop. The temperature demand was then ramped at 50°R/sec to design conditions. The behavior of the system during this ramp agreed extremely well with predictions as shown in Figure 14. The steady-state error during this ramp was between 40 and 50°R compared to a predicted error of 42°R. The ramp was prematurely terminated by power limiter action. This power limiting resulted from an error in calculating the power correction factor, and therefore, the power limiter setpoint, and was completely independent of the temperature control loop performance.

Oscillations of power and temperature occurred during EP-III, while operating at design conditions in the temperature control mode. These oscillations were caused by the temperature controller and temperature limiter responding to non-real temperature pulses seen on the average measured Station 26 temperature channel. The non-real temperature pulses resulted when one thermocouple, whose output was used as an input to obtain the Station 26 average temperature, failed to maximum output in a pulse manner. During the remainder of EP-III and EP-IV, the temperature controller performed satisfactorily and as expected.

The INIS system used on NRX-A5 proved quite satisfactory for use with the control system and the test data showed the INIS system to be more accurate than the water tank detectors. The INIS system performance is discussed in detail in Reference 8.

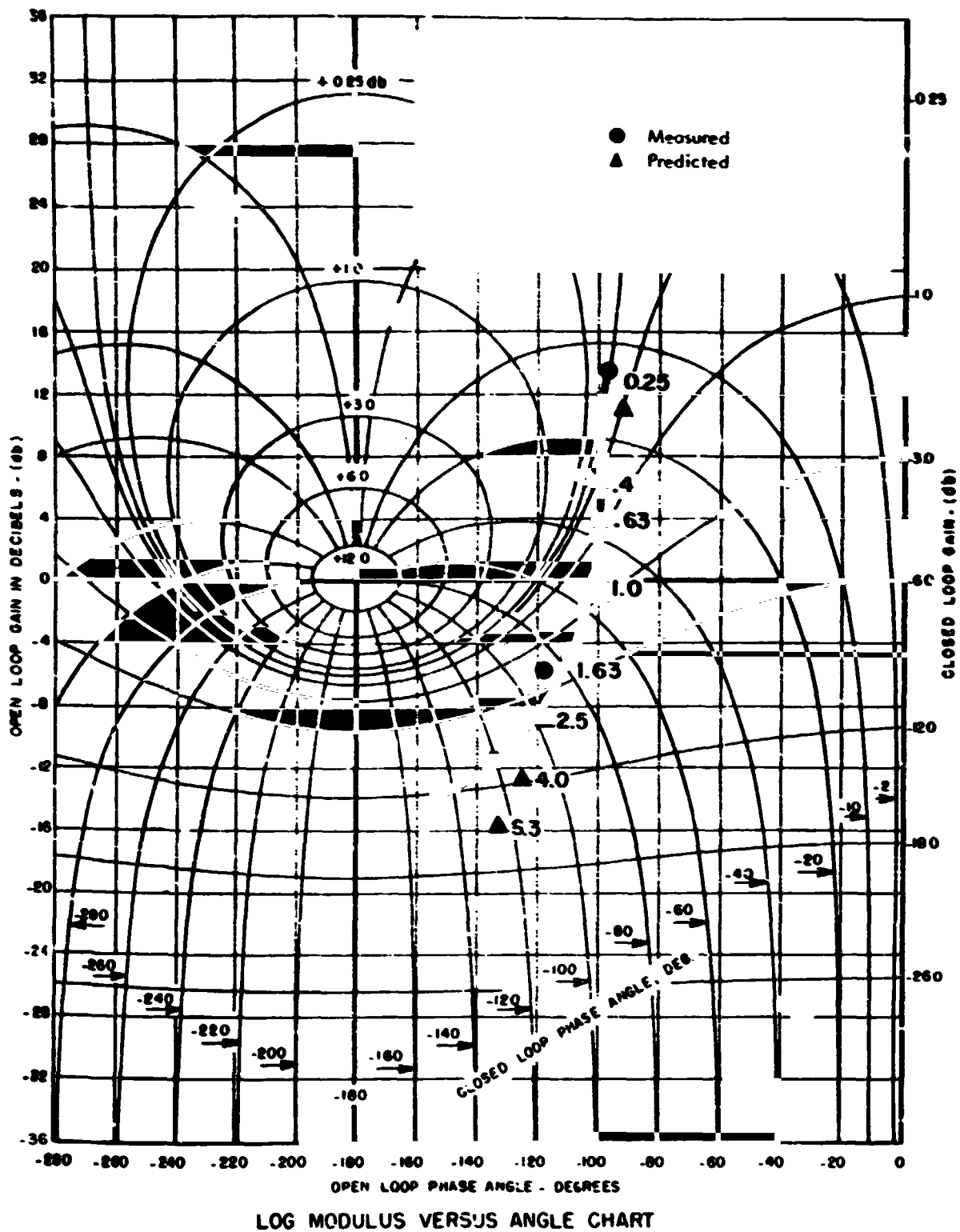


Figure 13. Measured Frequency Response of the Power Control Loop at 1 Kilowatt

~~CONFIDENTIAL~~

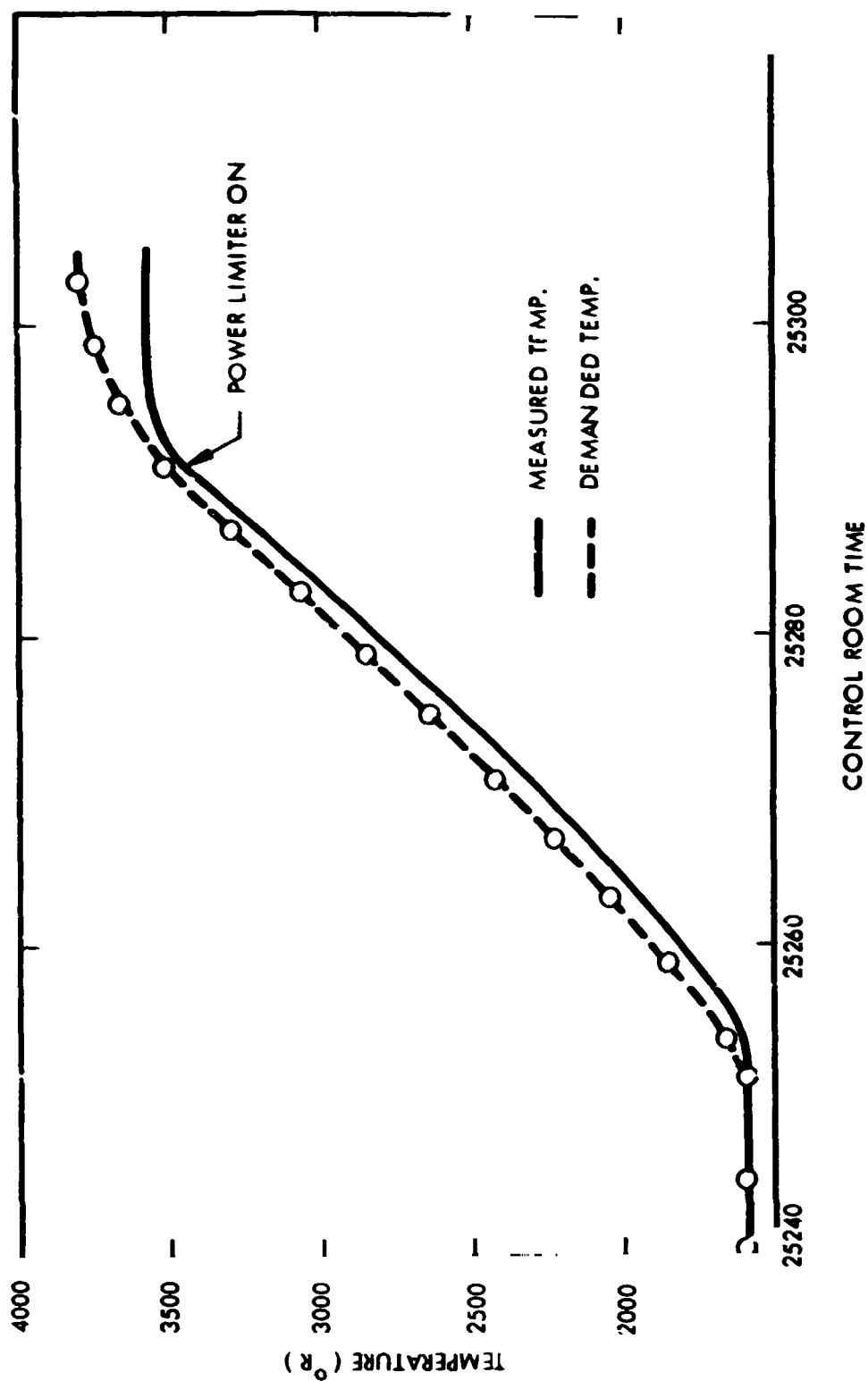


Figure 14. Station 26 Temperature Profile, EP-III Ramp from 2000°R Chamber Temperature to Design Conditions

~~CONFIDENTIAL~~

## 2.0 Feedsystem Control

The  $\text{LH}_2$  Flow and RPM Control System performed satisfactorily and as expected during the NRX-A5 tests. Typical comparisons of measured and predicted flow profiles for a ramp demand are shown in Figure 15.

The Specific Speed Control System operated properly during most of the test series. However, during the dynamic data experiments of EP-III, ACV-6 opened and remained open following the conclusion of this experiment. The opening of ACV-6 and venting of  $\text{LH}_2$  during the dynamics data experiments was not abnormal, but the valve should have closed when these perturbations ceased. The cause of this anomaly is believed to be either an error in the specific speed setting or loss of specific speed calibration, which would cause an inadvertent setting error possibility combined with a small error between measured RPM and the RPM signal seen by the specific speed controller.

## 3.0 Safety Systems

One anomaly occurred in the scram and flow shutdown chains during the NRX-A5 test series. This anomaly was an erroneous floating power scram which occurred during EP-III. Since this input was by-passed at the time of the anomaly, the erroneous floating power scram had no effect on system operation. The cause of the anomaly was an open resistor in the electronic equipment feeding the scram chain.

Checkout of the velocity mode and fixed drum mode power limiters was performed following the neutronics calibration phase of EP-II. Both modes of power limiters showed satisfactory transient response and stability during this checkout.

The velocity mode temperature limiter was checked out during EP-III at a Station 26 temperature of  $1500^\circ\text{R}$ . This checkout assured the stability of the velocity mode temperature limiter and compared favorably with predictions. The combined checkout of the power and temperature limiters operating together in both the velocity and fixed drum modes was performed during the full power hold of EP-III. Again, the limiter action during the transient was stable and essentially as predicted.

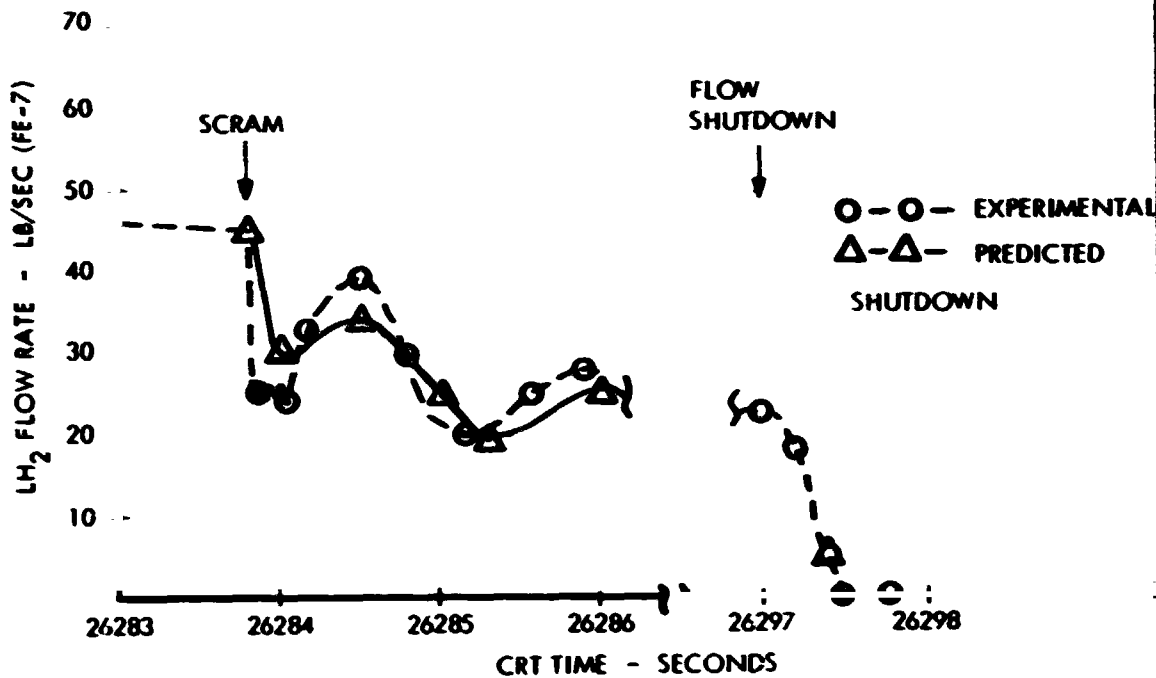
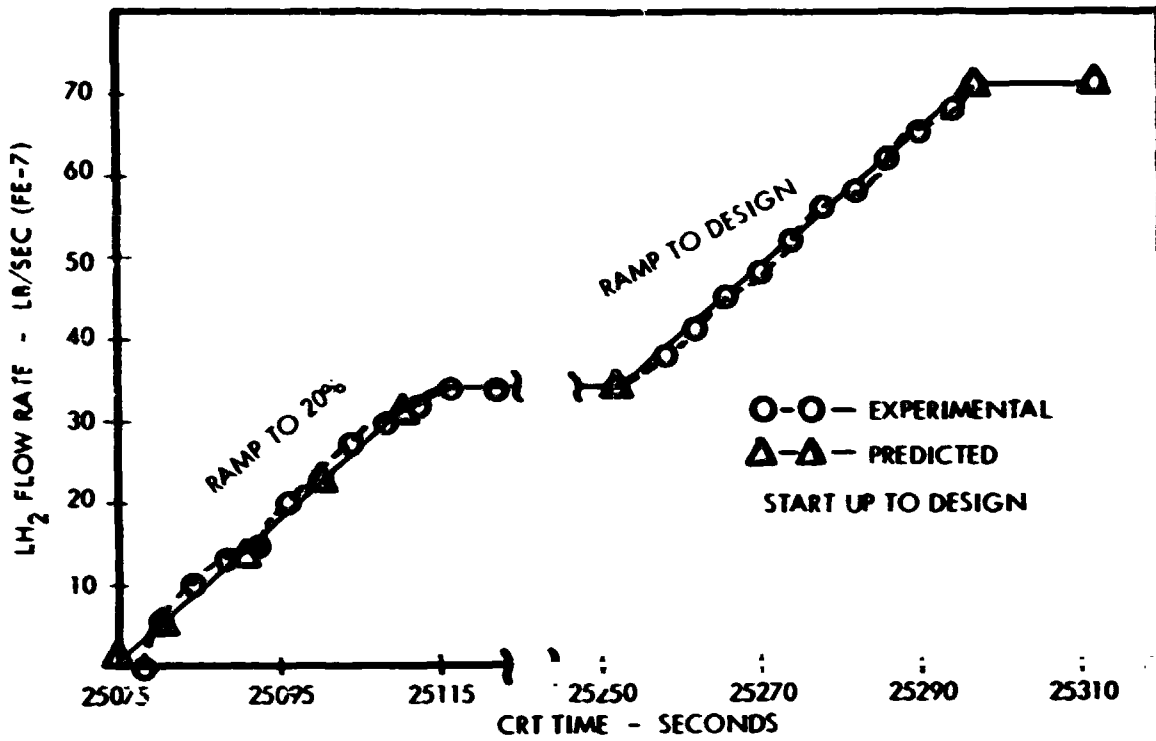


Figure 15. Pump Outlet Flow Rate Profile for EP-III



No conditions occurred during the NRX-A5 tests which required the operation of either the power or temperature inhibitors.

The scram flow tailoff system was used during the scrams which terminated EP's III and IV. The primary differences between the measured transients and predicted transients was that the actual flow decreased faster than had been predicted and the pump speed was greater than predicted. These differences were the result of the initial position of ACV-6. The design and predictions assumed the valve to be closed at the time of scram; whereas, the test data showed the valve to be 10 percent open at this time. However, these differences resulted in no problems nor required any change in the system design. During the scrams, the scram flow tailoff system met the primary design constraints of satisfactory thermal transients and prevented the pump from operating in the stall region. The NRX-A5 scram flow tailoff system reduced flow much more rapidly than it had been reduced on any prior test series.

The  $\text{GH}_2$  control system was checked out by obtaining system response to step inputs. These checkouts displayed in Figure 16 show close agreement with predicted performance. The  $\text{GH}_2$  control system performed as predicted during the flow shutdowns of EP-III and EP-IV.

#### G. DOSIMETRY

During the testing of the NRX-A5 reactor, a dosimetry program was carried out which resulted in the measurement of gamma ray dose rates, fast neutron fluxes ( $E > 2.9 \text{ Mev}$ ), and thermal neutron fluxes ( $E < 0.4 \text{ ev}$ ) at 57 locations external to the reactor. Since the NRX-A5 reactor test configuration was very similar to the previously tested NRX reactors, the philosophy of the dosimetry program was to obtain data which would both supplement previously measured data and reduce the uncertainty in gamma and neutron data measured during the NRX-A2, NRX-A3, and NRX/EST reactor tests. Although the NRX/EST reactor was run in a different facility environment, there were areas around the NRX/EST which had the same radiation environment as the NRX-A5 reactor; where this was the case, the NRX/EST data are included for comparison.

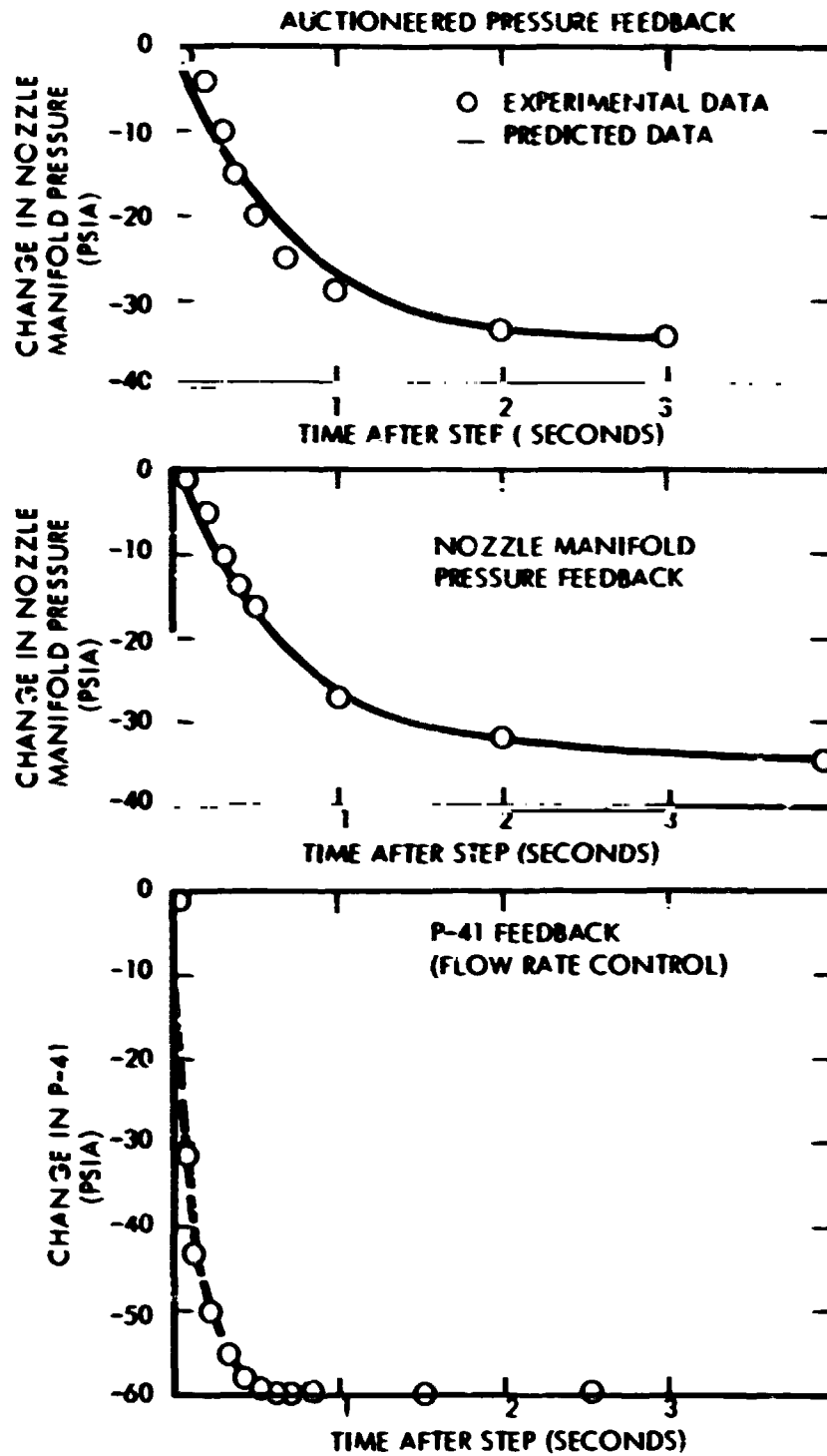


Figure 16. PCV-41 Step Responses During EP-1



Based on the NRX-A2 through NRX-A5 dosimetry test data, along with calculations where needed, typical radiation patterns around an NRX reactor in Test Cell "A" were determined. The data are presented in the form of iso-flux contours for fast neutrons, iso-dose rate contours for gamma rays, and iso-heating rate contours for radiation heating in aluminum. These data, which are presented in Figures 17, 18, and 19, respectively, are considered to be accurate, generally, to within a factor of two.

Fast neutron fluxes ( $E > 2.9$  Mev) were obtained using sulfur pellets. Thermal neutron fluxes ( $E > 0.4$  ev) were also measured using bare and cadmium-covered gold foils. Both the fast and thermal neutron flux data are in good agreement with similar data obtained during the previous reactor tests where comparisons are valid.

Gamma ray dose rates were measured using both thermoluminescent detectors and silver metaphosphate glass detectors. At locations close to the reactor, i.e., up to five feet from the center of the core, the NRX-A5 measurements were in reasonable agreement with previously measured gamma ray dose rates. In general, the gamma ray data obtained at greater distances were found to be less reliable than that obtained from the earlier reactor tests. This can be attributed to the uncertainties in the high gamma ray background at the test facility produced by the accumulation of residual activity from the testing of previous reactors.

#### H. POST-OPERATIVE RADIOCHEMISTRY

Following the NRX-A5 power test, the integrated radial and axial fission distribution was established by gross radiation measurements and radiochemical analysis (Reference 19). As in the NRX/EST post-operative analysis, a comparison of these NRX-A5 measurements with predictions was more difficult than in NRX-A2 and NRX-A3 due to the high loss of material from the fuel elements during the test.

An effective drum angle of 119 degrees was obtained for the entire test profile, enabling the calculated power distribution to be compared directly with that derived from the gross radiation measurements. Prior to comparison, the activity measurement for each

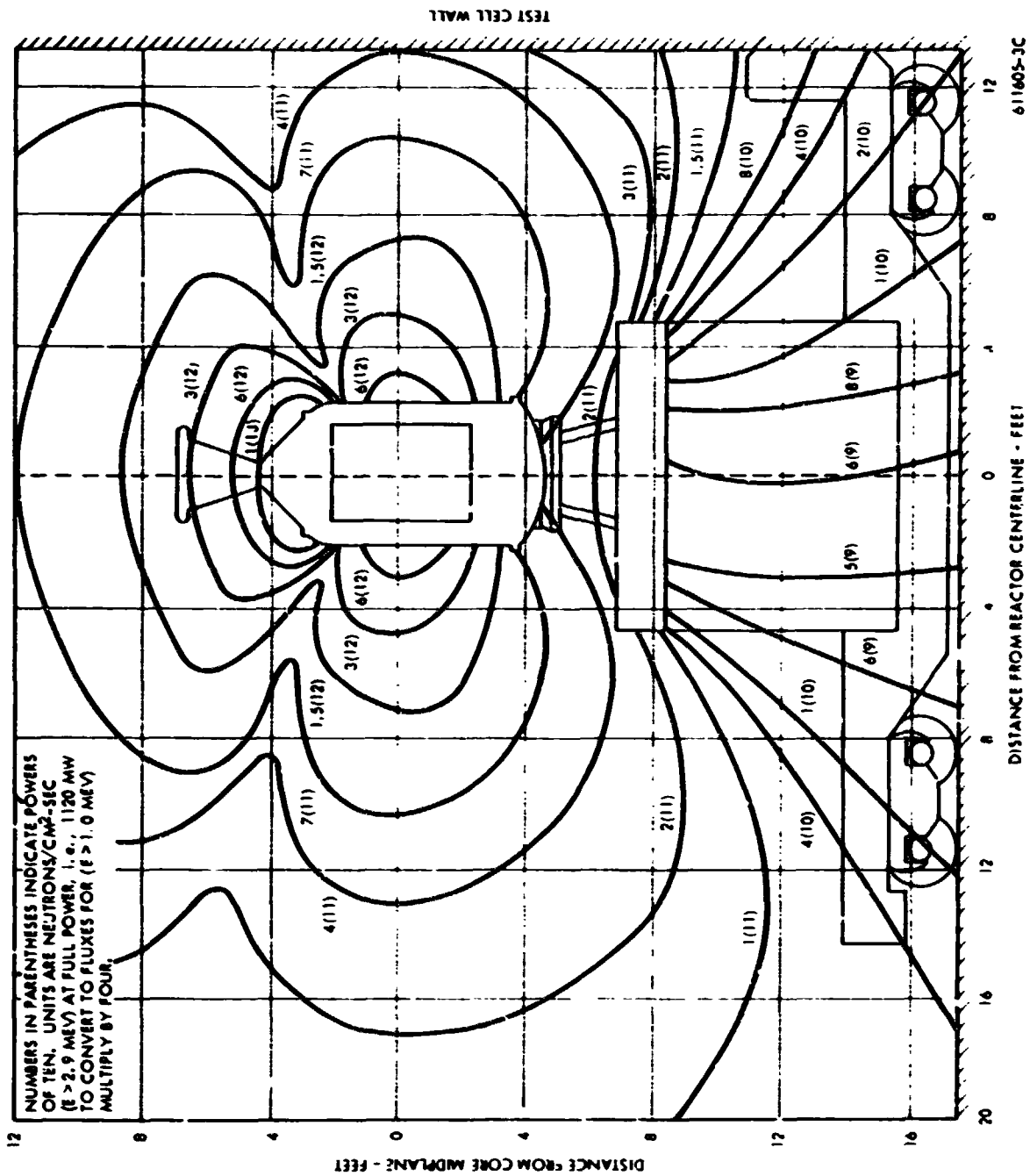


Figure 17. Fast Neutron ( $E > 2.9$  Mev) Iso-Flux Pattern Around a Typical NRX Reactor in Test Cell "A"

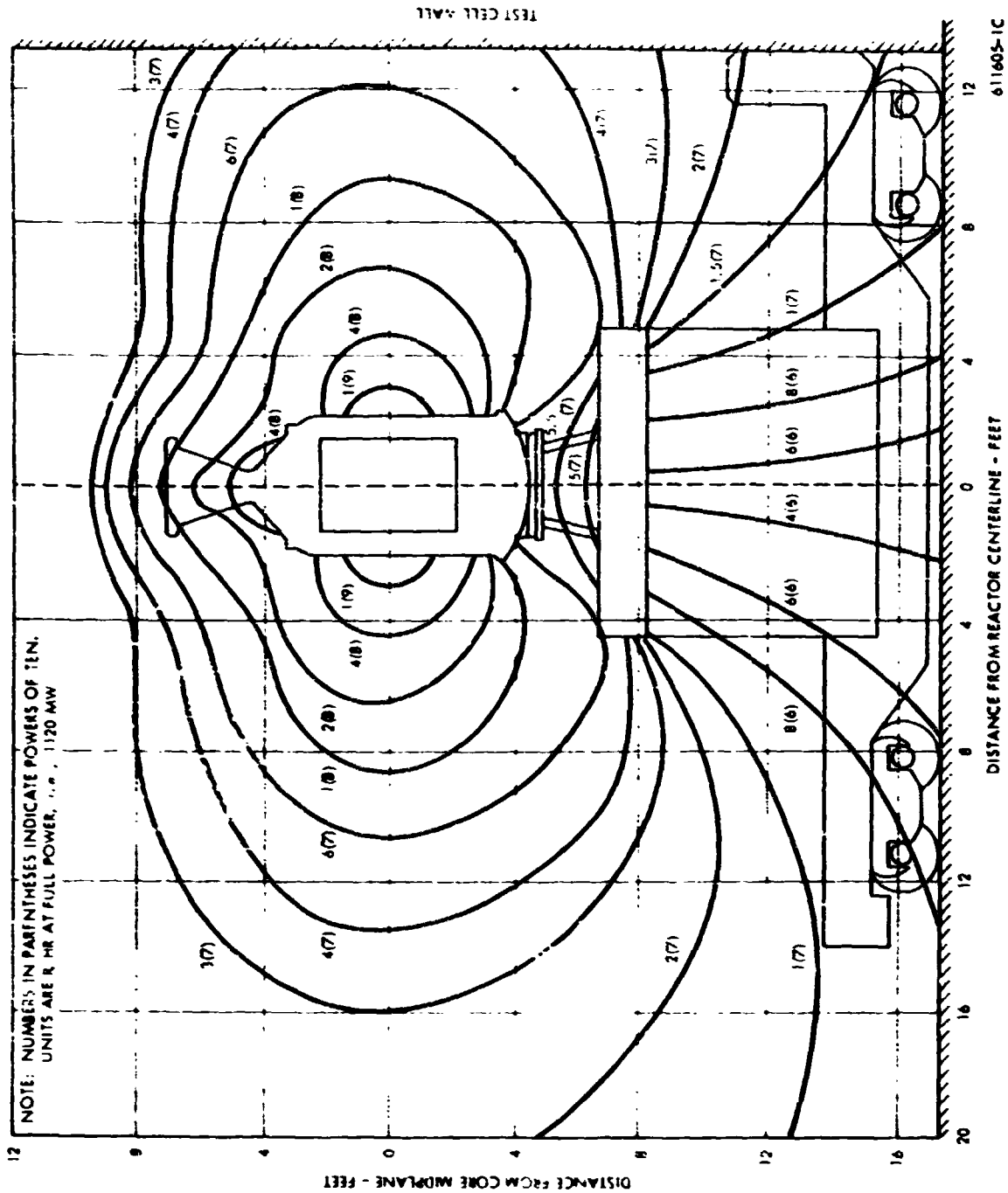


Figure 18. Gamma Ray Iso-Dose Pattern Around a Typical NRX Reactor In Test Cell "A"



49

**CONFIDENTIAL**

element was adjusted to account for the reduction in intensity associated with loss of fission products by corrosion. Three independent methods were used to derive this correlation. The first method utilized the change in activity as a function of weight loss for elements from a given location, but in different core sectors. The effects of corrosion were also estimated by analyzing individual element deviations, from a trend in the ratio of the experimental to predicted fissions per gram values in the integrals of the measured and predicted axial power distributions in fuel elements with large weight losses.

A comparison of the adjusted experimental fission product activity with the 119 degree effective drum angle prediction shows a maximum difference of 4.7 percent on a per element basis. The differences noted were due mainly to design differences between the NRX-A5 and NRX-A3 reactors, since the prediction was based on the NRX-A3 test results. PAX power measurements have since shown that the fuel loading differences between the two reactors would cause power changes of as much as 5 percent. Smaller errors than this were introduced by the code 32 element power perturbations that were applied to the predictions. Recent PAX-E peripheral power measurements (Reference 20) which mapped the complete core boundary, both with fueled and unfueled partial elements, have since shown that these perturbations were slightly underestimated.

The NRX-A5 predicted axial power distribution showed good overall agreement with the gamma scan measurements. This agreement was similar to that seen in the NRX-A3 analysis (Reference 21).

A comparison of the cold PAX-D power distribution and that derived from the NRX-A5 post-operative ionization measurements indicated little or no difference in the cold and hot power distributions except in the edge fuel elements where the observed cold-to-hot power change showed a definite rise. This cold-to-hot power swing is slightly more pronounced than observed from the NRX/EST data (approximately 2 percent).

**CONFIDENTIAL**

~~CONFIDENTIAL~~



## VI. POST-OPERATIVE EXAMINATION

The NRX-A5 Test Assembly was returned from Test Cell "A" and placed in the Disassembly Bay of the R-MAD Building on July 6, 1966. Disassembly was initiated at that time and continued until approximately September 1, 1966, at which time all subassemblies had been dismantled. Post-operative examinations took place in the Disassembly Bay and the R-MAD hot cells, with some non-fueled mechanical tests, fuel element examinations, and metallographic examinations being performed at LASL, Wing 9 of CMB-14.

A general evaluation is given in summary form in the following paragraphs for the major components composing the NRX-A5 reactor assembly.

### A. OUTER REFLECTOR SECTORS

The condition of the Outer Reflector Sectors was good. All sectors were dye checked for possible cracking of the webbed areas. No indication of cracks was observed on any sector. Dimensional measurements obtained on four sectors showed no significant changes from pre-operational dimensions.

### B. INNER REFLECTOR AND SUPPORT SYSTEM

The NRX-A5 design incorporated a new axial support system combined into one assembly to facilitate handling and to provide axial motion limits. This function was formerly provided by the aluminum barrel which was eliminated from this reactor. The graphite cylinder was modified to be compatible with this axial support system and improved lateral support system. In addition, an improved method of retaining the nozzle end seal was incorporated, and the impedance ring was relocated to increase the margin of safety of the inner reflector cylinder. All components of the inner reflector system and support performed satisfactorily.

### C. HOT BUFFER FILLER STRIPS AND TILES

An extensive amount of breakage and corrosion occurred to filler strips installed in the hot buffer region of the core. A total of thirty-nine of the fifty-four hot buffer strips

~~CONFIDENTIAL~~



contained breaks in one or more of the following areas: (a) nineteen strips contained breaks at the forward end at the cut-out for the core band and fuel element key; (b) twenty-six filler strips contained breaks between Stations 20 and 49; (c) five strips contained breaks at the aft end 1/4 inch with subsequent loss of the tile retaining ledge. The hot buffer filler strips experienced a substantial amount of corrosion both on the inside faces of the strips where they contacted the fuel elements and on the radial faces between adjacent strips. The material loss occurred in the form of rivulets of randomly varying width and depth, beginning at about Station 22 and extending to the coated end of the strip. The deepest corrosion occurred on the lateral faces at the outer diameter. Observations from the flow patterns on the filler strip surfaces indicated a considerable amount of in-flow at the hot end. Figure 20 is representative of the filler strip surface regression in the hot buffer region. Mild surface attack and sooting was observed in some cases as far upstream as Station 12 with increasing severity toward the aft end of the strips. A detailed view of corrosion present in the downstream portion of representative hot buffer strips is shown on Figure 21. Corrosion depth of the radial faces varied somewhat randomly, but corrosion was particularly severe in the region between Stations 46 and 50 near the tile retaining lug.

The appearance of filler strip breaks indicated that they occurred in regions which were initially weakened by corrosion, and it was suggested that the breaks had occurred during the latter stages of the test run. Corrosion was generally absent in the coated region of the filler strips except where regression of the adjacent radial face had produced undercutting of the coated surface, with subsequent overhanging or flaking of the NbC. Small pieces of graphite broken from the forward ends of the hot buffer filler strips were believed responsible for blocking orifice and cluster plate channels of the 5F5 cluster. This resulted in overheating and subsequent damage to both 5F4 and 5F5 components.

In addition to breakage of hot buffer filler strips, approximately ten (10) hot buffer tiles were broken in the aft end retention notch. The tiles sustained mild corrosion and sooting along edges and on filler strip contact surfaces. This corrosion condition was observed on tiles as far upstream as Station 12. The appearance of the filler strip region, at the junction of the

**CONFIDENTIAL**

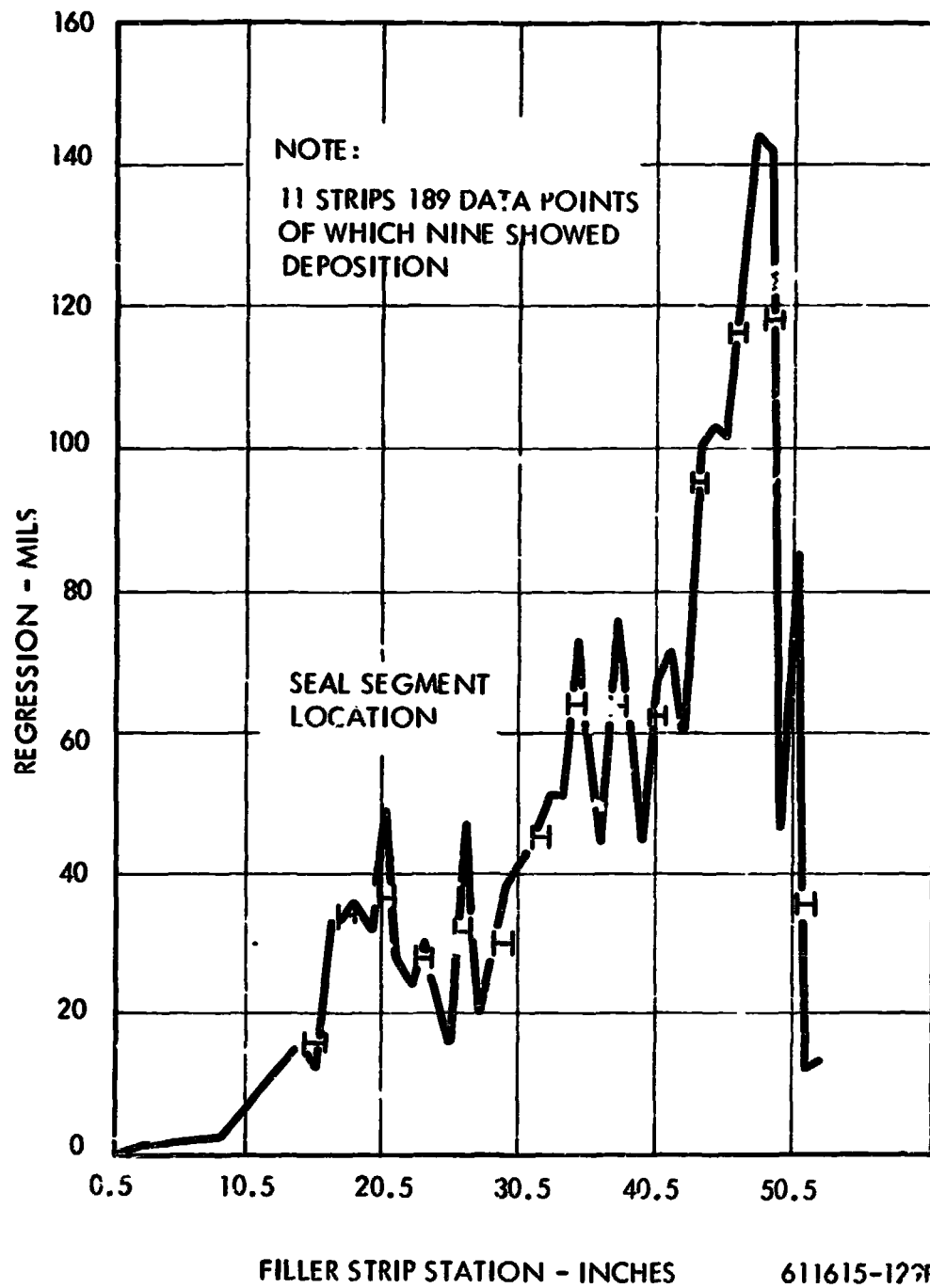


Figure 20. Filler Strip Surface Regression In Hot Buffer Area

**CONFIDENTIAL**

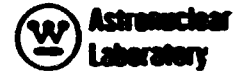
~~CONFIDENTIAL~~



Figure 21. Hot Buffer Filler Strip Corrosion

~~CONFIDENTIAL~~

~~CONFIDENTIAL~~



hot buffer and nominal filler strip sectors, is shown in Figure 22.

#### D. NOMINAL FILLER STRIPS AND TILES

The equivalent of four sectors of nominal filler strips was installed in NRX-A5. These strips were similar to those in NRX/EST, except that the fifteen short forward tiles which contacted the fuel element were replaced by a single full-length tile which was added to minimize gaps and plenums in the core periphery. The filler strips were, generally, in good condition but sustained some mild sooting and showed a regular pattern of seal segment bearing marks on strip peripheral surfaces as noted for previous reactors. Light corrosion was present on the sides of some strips, tending to be somewhat heavier toward the aft end of the strips. In general, both NRX-A5 long filler strip tiles and filler strips sustained less corrosion than was observed for the NRX/EST counterparts.

#### E. FILLER BLOCKS

The filler block length for NRX-A5 had been shortened to provide more axial clearance between the blocks and filler strips in order to prevent the interference and breakage of the band retaining lugs. There was some chipping of a few of the filler blocks in the vicinity of the band retaining lugs. However, as there was no indication of interference with the filler strip, this chipping was attributed primarily to disassembly operations.

#### F. SUPPORT BLOCKS

Design of the NRX-A5 support blocks differed slightly from the design of NRX-EST support blocks in that the aft counterbore fillet radius was increased in order to eliminate the cracking and corrosion observed in this area for NRX/EST. In addition, a coated ATJ graphite support washer was used with ten pyrofoil washers compressed between the support washer and the counterbore seat to give a more uniform load distribution on the block. The pyrofoil washers additionally served to reduce leakage of hydrogen, in the event of occurrence of counterbore cracks.

The condition of the NRX-A5 regular support blocks (those having six symmetrical lobes) was generally better than that of the NRX-EST blocks, with only minor corrosion,

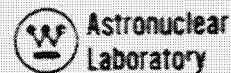
~~CONFIDENTIAL~~



Figure 22. Nominal and Hot Buffer Filler Strip Design Interface



**CONFIDENTIAL**



flaking and crazing encountered in most cases. Foreward end support block corrosion, where present, was generally related to heavier than normal upstream fuel element corrosion, and was most prevalent in the central and outer regions of the core. Examination of several sectioned blocks showed no evidence of counterbore cracking or associated corrosion as was noted for NRX-EST regular support blocks. The appearance of a typical regular support block, and a skirtless support block is shown in Figures 23 and 24, respectively.

NRX-A5 irregular support blocks (those having more than six lobes, or that are unsymmetrical), were also in better condition than NRX-EST irregular support blocks, due to the reduction of cracking and foreward face corrosion. There was, however, some axial cracking of the skirt of most irregular blocks, as well as transverse cracking of the J-9 configuration blocks. To reduce this problem in NRX-A6 and XE-1, the partial lobes of the J-3, J-5 and J-9 support blocks were removed.

Weight loss data for blocks was correlated with surface coating appearance. Blocks with good to excellent performance showed an average weight loss of about 1.43 percent. Blocks which exhibited severe crazing and/or flaking had an average weight loss of about 2.13 percent. In all cases, higher weight losses were associated with specific areas of damage, and were not the result of uniform weight loss. Poor performing blocks were, in general, associated with specific coating runs. As indicated previously, massive fuel element damage resulted in poor block performance.

The NRX-A5 contained six experimental skirtless support blocks to verify the adequacy of the block with the aft end skirt eliminated. The blocks performed satisfactorily; however, two of the blocks suffered moderate forward face damage as a result of fuel element deterioration upstream of the blocks.

The ATJ graphite protection cups which replaced the skirted portion of the skirtless blocks, were also in good condition. Although there was evidence of crazing and some loss of coating due to flaking, there was no apparent corrosion of the protection cups.

**CONFIDENTIAL**



~~CONFIDENTIAL~~

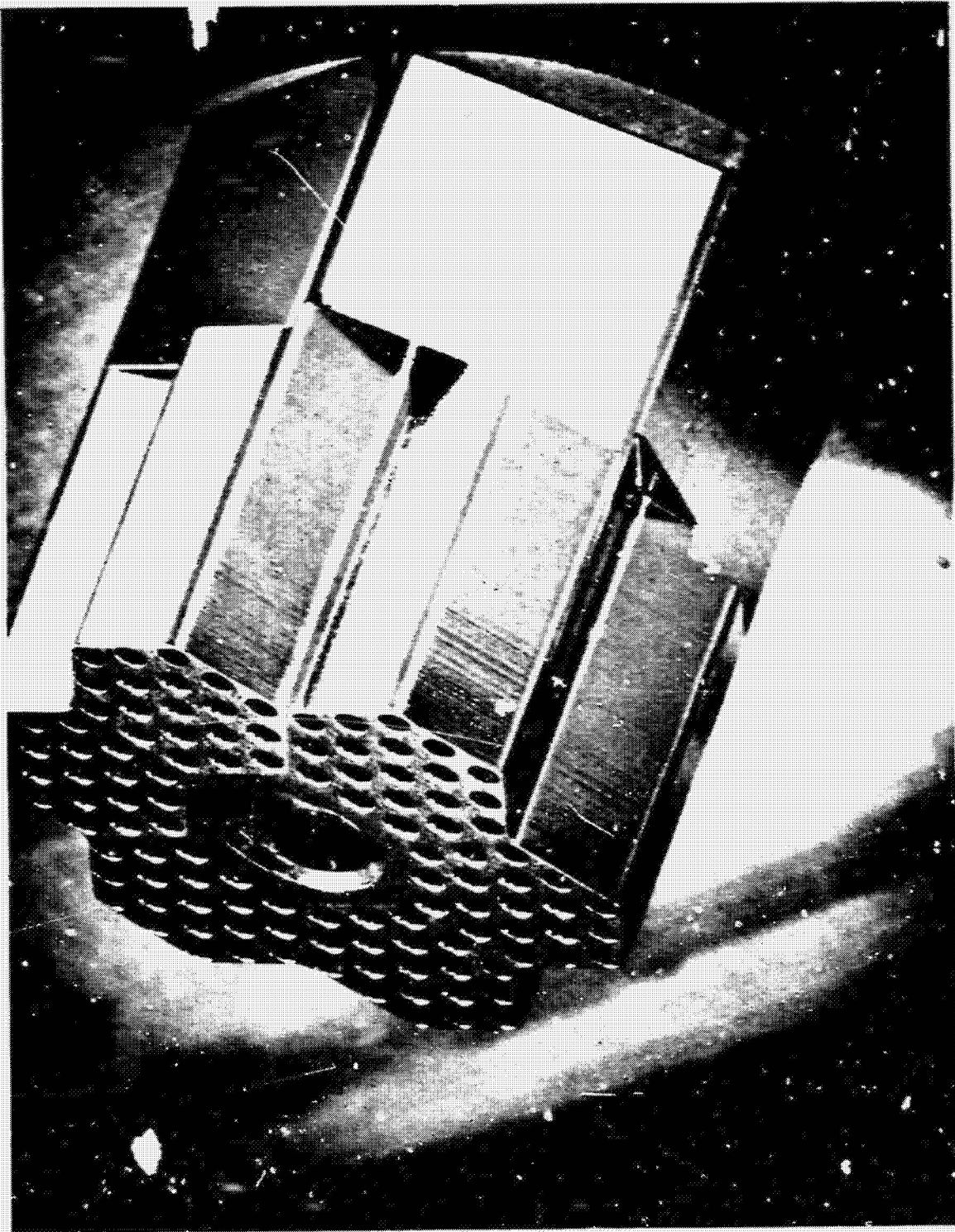


Figure 23. Regular Support Block

~~CONFIDENTIAL~~



~~CONFIDENTIAL~~

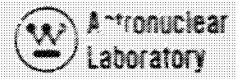


Figure 24. Skirtless Support Block

~~CONFIDENTIAL~~



The over-all performance of the NRX-A5 support blocks including both mechanical and corrosion performance was better than for previous reactors. This was attributed, in part, to the absence of the extended low power runs, mapping cycles, and a lower startup ramp rate, 60 degrees R/sec maximum compared to 150 degrees R/second for NRX/EST.

#### G. LINER TUBES

All liner tubes examined (except 5F5) were in good condition. As in NRX/EST and previous reactors, many of the tubes contained discolored bands in locations corresponding to the insulating sleeve interfaces. These discoloration bands generally were present on the forward half of the liner tube and absent on the hotter aft end. Several of the tubes examined exhibited a slight flaring condition at the aft end, as was previously noted on several NRX/EST liner tubes. No evidence of high temperature reaction (carbiding) between the liner tubes and the graphite insulating sleeves was observed.

#### H. INSULATING SLEEVES

The insulating sleeves were in relatively good condition. Generally, slight corrosion was present on the last five or six sleeves from the hot end of the cluster, resulting in rounding in some cases of the outside corner at each end of the sleeve. However, a close fit was still provided between adjacent sleeves. This condition was accompanied by general sooting on the outside of the sleeves. The upstream sleeves were in excellent condition.

#### I. SUPPORT WASHERS

The NbC coated ATJ graphite support washers were in excellent condition with the coating intact and with little or no evidence of corrosion. The pyrofoil washers which were sandwiched between the support washer and support blocks were generally in good condition, although many had experienced corrosion of varying degrees on the outside diameter.

#### J. TIE RODS

The tie rod material for NRX-A5 was Inconel 718 rather than Inconel 750 employed for previous reactors. Seven hollow Inconel 718 tie rods were included in the core assembly.

~~CONFIDENTIAL~~



The hollow tie rods contained thermocouples for directly measuring tie rod material temperatures.

In general, the tie rods were in excellent post-test condition, although some surface discoloration was typically present on all but the fore and aft two to four inches.

Room temperature tests were performed on samples representing a cross-section of the tie rods. For comparison, nine un-irradiated control samples were similarly tested. The tensile tests revealed the following general trends:

- (1) The hollow tie rod samples were significantly stronger than the solid tie rod samples, for both the post-test and control (pre-test) cases. The hollow tie rod samples were also characterized by a grain structure different from that of the solid tie rod samples, indicating a different processing history, which probably resulted in the increased strength.
- (2) The strength of the Inconel 718 tie rods was significantly greater than that of the Inconel 750 tie rods previously used, for both the post-test and pre-test cases. Tensile samples from the forward end of the tie rods were stronger than samples removed from the aft end. Presumably, this effect was the result of fabrication rather than irradiation exposure, since control samples were similarly affected.
- (3) One sample showed low elongation, rather low yield strength, and 20 to 30 KSI lower ultimate strength than comparable specimens. This sample was from the aft end of tie rod 5F5, the cluster which sustained heavy corrosion and localized melting of the liner tube as a result of orifice plugging.
- (4) There was some indication that tie rods in the central region of the core sustained a more pronounced change in properties than was sustained by peripheral cluster tie rods. However, property changes, even in 5F5, were not sufficient to cause concern.

K. DAMAGE TO THE 5F5 CLUSTERS

Six fuel elements in these two clusters were badly damaged and sustained corrosion to the extent that reliable weight loss data could not be obtained. Element 5F5C, which

~~CONFIDENTIAL~~

sustained the most damage, was severely corroded as far upstream as Station 14. A substantial portion of the aft ends of several other elements was missing, although the forward undamaged ends had not moved downstream from their original positions. The central element of cluster 5F5 was severely corroded between Stations 34 and 48, and the pyrolytic graphite sleeves were exposed. At Station 42, which coincides with a pyrolytic graphite sleeve joint, the underlying stainless steel liner tube was melted through as shown on Figure 25. However, the tie rod was intact and showed no evidence of physical damage, with the exception that a small blob of molten metal from the liner tube had adhered to it.

The support blocks for both 5F4 and 5F5 clusters were also badly corroded. Lobes on both blocks were partially missing in the vicinity of the severely corroded fuel elements, but were intact in the region of undamaged elements. Although three (3) lobes of the 5F5 support block were extensively damaged, the counter bore area and all support hardware were in excellent condition, retaining their load carrying capability.

The extensive corrosion described above was attributed to blockage of coolant flow by pieces of graphite broken from the forward ends of hot buffer filler strips. Cluster plate orifice plugging was observed in the 5F5 cluster plate and two additional pieces of graphite were observed blocking orifices of fuel element 5F5 C, as shown on Figure 26. The resulting severe overheating accelerated corrosion in the 5F5C element, which then produced corrosion in adjacent elements by increasing flow around the unprotected external surfaces. Even though the elements in this region were severely corroded, there was no indication that the support blocks, tie rods, and associated hardware were not performing their intended design function.

#### L. INSTRUMENTATION

Post-test instrumentation measurements were made to determine the electrical condition of installed sensors and their connections into the test cell. In most cases, post-test measurements were within  $\pm 2\%$  of pre-test measurements. Where greater changes were experienced, they were generally believed to be due to higher post-test ambient reactor temperatures.

~~CONFIDENTIAL~~

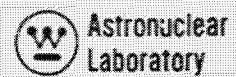


Figure 25. Severed Liner Tube, SF5 Cluster, Station 42

~~CONFIDENTIAL~~

~~CONFIDENTIAL~~

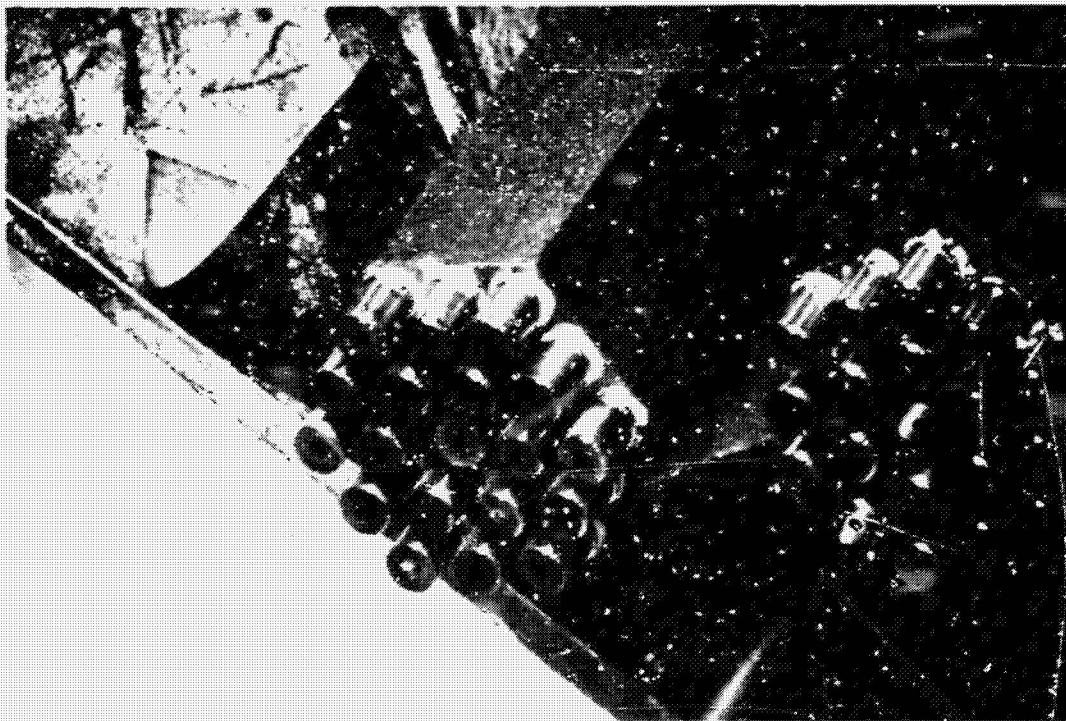
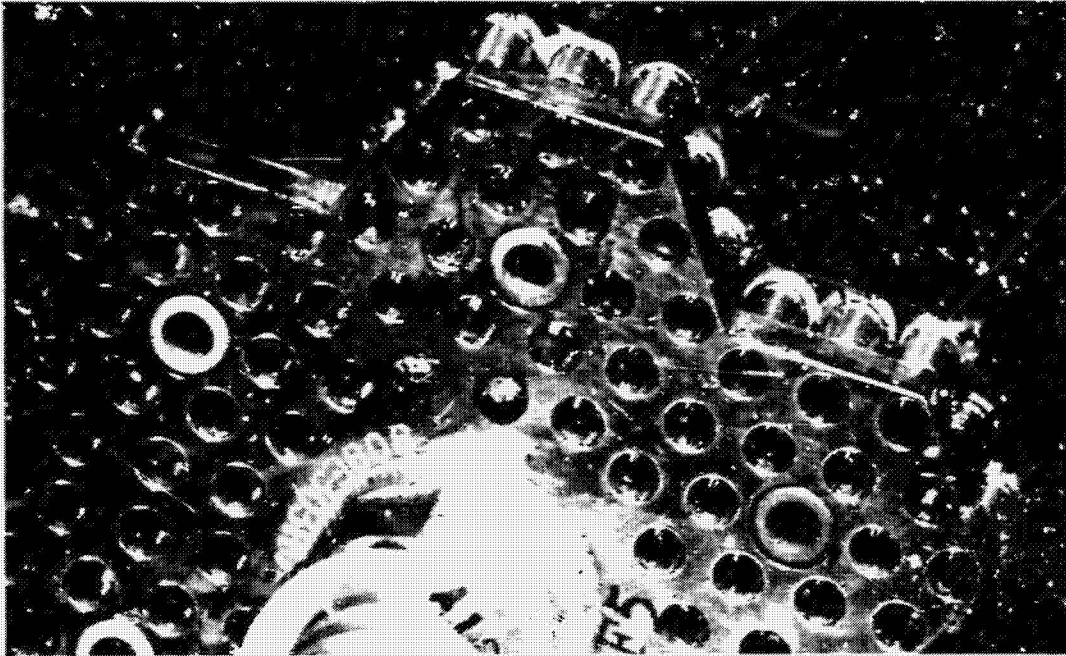


Figure 26. Blocked Orifices, 5F5 Cluster Plate and 5F5C Fuel Element

~~CONFIDENTIAL~~

In general, performance of the WANL supplied diagnostic and control sensors was excellent, and 95% of the sensors remained operational at the conclusion of all testing. Most of the sensor failures encountered during testing were verified by conditions observed during the post-test electrical check, or other post-operational phases.

#### **M. CONCLUSIONS**

Although the general performance of most NRX-A6 Reactor Components was satisfactory, the need for continued development to increase core life was pointed out for the following areas:

- (1) Improvement in graphite coating technology, with emphasis on fuel element bore coating improvement.
- (2) Elimination of filler strip breakage in the hot buffer filler strips.
- (3) Improvement in protection against corrosion for the ends of the conventional filler strips.
- (4) Elimination of corrosion problems at the core periphery.
- (5) Study and elimination of the peripheral element cracking problem.
- (6) Reduction in thermal stresses in the support blocks, and improvement in block coating techniques.
- (7) Improvement in insulating sleeve joint design, to offer further protection to the tie rod under abnormal operating conditions.

**BLANK PAGE**



~~CONFIDENTIAL~~



## VII. FUEL ELEMENT PERFORMANCE

The major damage associated with the NRX-A5 reactor was, as in the case of previous reactors, corrosion of the fuel elements and the core support components. A view of the aft end of the NRX-A5 core is shown in Figure 27. The darkened area in the center of the core (clusters 0-00 through Row D) is due to excessive pyrolytic carbon, "soot", deposits on support block surfaces, and is indicative of high weight losses to fuel elements positioned upstream. The location of the six skirtless support blocks and the 5F4 - 5F5 support block lobe damage discussed previously is also shown on Figure 27. The major categories of damage to fuel elements observed in NRX-A5 may be listed as follows:

### A. BREAKAGE

Forty-two percent of the elements in the NRX-A5 core were observed to be broken upon removal from the core. The central (0-00 through D clusters) and peripheral regions (H and J clusters) sustained most of the breaks. These regions also sustained the greatest element weight loss. The central and peripheral regions were made up of essentially WAFF elements, and the intermediate region contained nearly all Y-12 elements. It was noted that the fuel element breaks appeared to be of two distinct types, (1) elements that broke as a result of loss of strength due to reduction in cross sectional area by channel enlargement; and (2) elements that were partially or completely cracked through and sustained significant corrosion in the area of the crack. Breakage of the second type was more prevalent in the peripheral region, while breakage of the first type was more prevalent in the central region of the core. Examples of the two types of fuel element fractures are shown in Figure 28.

### B. WEIGHT LOSS

A total of 1584 fuel elements were contained in the NRX-A5, of this total 1551 were weighed. Elements which were not weighed were assumed to be broken and unidentifiable. A summary of the measured weight loss data is given in Table 2, which includes an average assumed post-test weight for all unweighed elements. The implied average overall weight loss,

~~CONFIDENTIAL~~



**CONFIDENTIAL**


Table 2  
NRX-A5 Total Fuel Element Weight Loss

	WAFF	Y-12	All
Total No. of Fuel Elements in Core	839	745	1584
Total No. Intact Elements Weighed	252	673	925
Total No. Broken Elements Weighed	562	64	626
Fraction Broken	.700	.097	.416
No. of Unweighed Elements	25	8	33
Average Weight Loss - Intact Elements (gms)	20.8	14.4	16.2
Average Weight Loss - Broken Elements (gms)	43.8	30.5	42.4
*Implied Average Weight Loss - All Elements (gms)	30.9	16.0	27.0

\* Assuming that unweighed elements are broken and equal in weight to the average for weighed broken elements.

**CONFIDENTIAL**

**CONFIDENTIAL**

 Astronuclear  
Laboratory

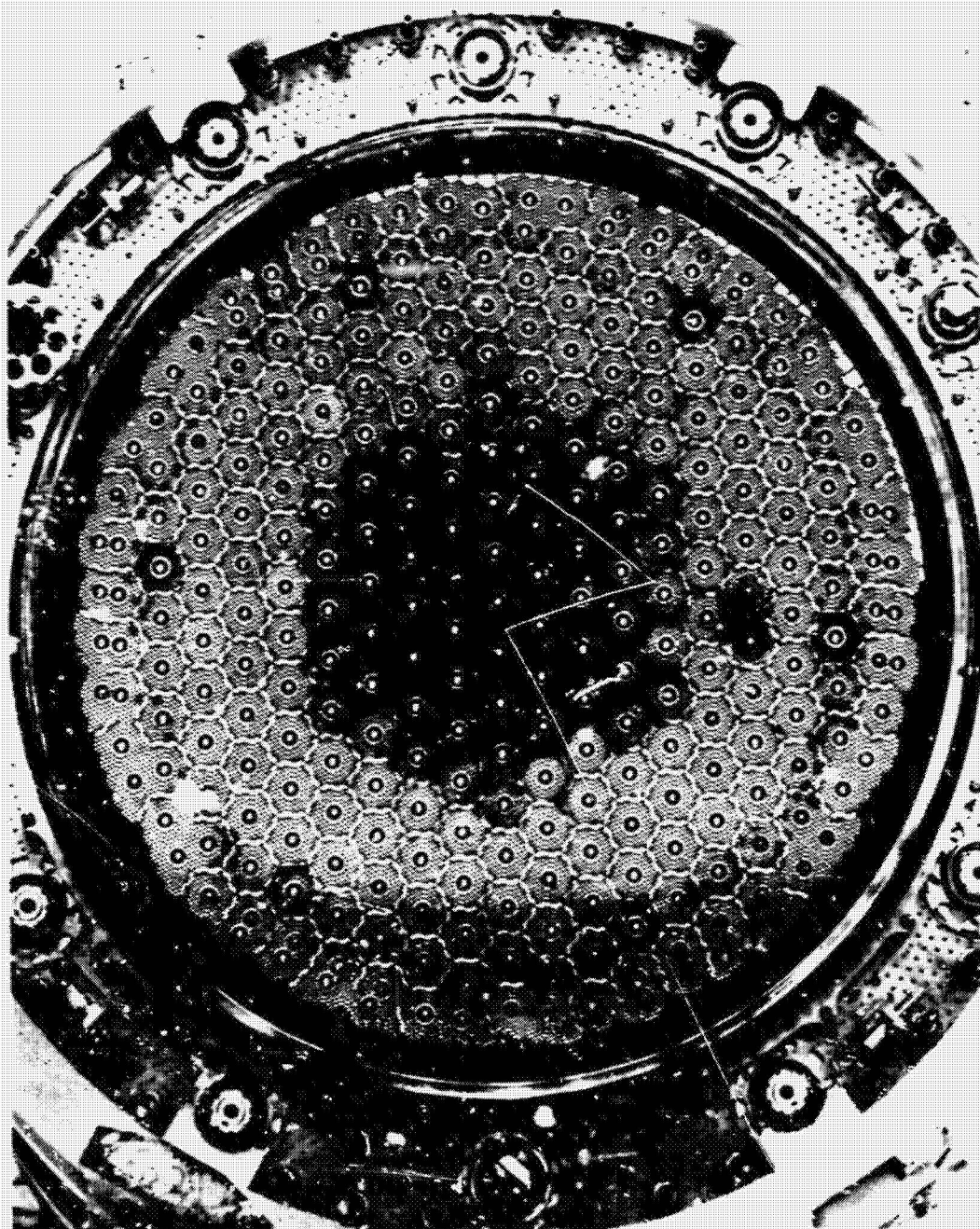


Figure 27. NRX-A5 Core Exit, Showing Sooting Patterns

**CONFIDENTIAL**

~~CONFIDENTIAL~~

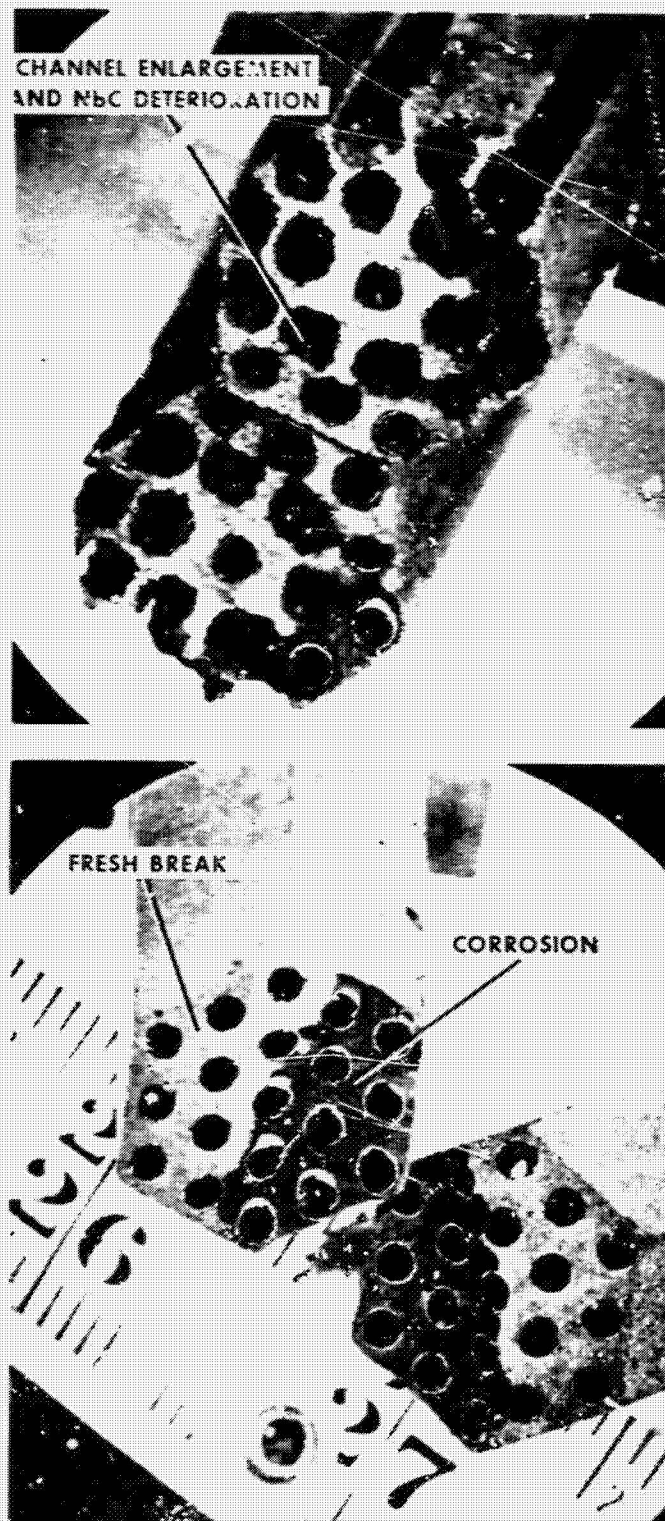


Figure 28. Fuel Element Breaks

~~CONFIDENTIAL~~

~~CONFIDENTIAL~~



based on measurements of 925 unbroken and 626 broken fuel elements, was 27.0 grams per element, with a total core weight loss of approximately 43 kg. The average WAFF element weight loss in NRX-A5 was approximately 36.9 grams/element and the average Y-12 element weight loss was 16.0 grams/element. In comparison, the fuel element weight loss for NRX/EST averaged 32.2 grams/element. In general, the higher weight losses occurred at the core central and peripheral regions, with a relatively low weight loss in the mid-radial region, approximately 8.0 to 13.0 inches from the core center. A significant difference in weight loss occurred to both WAFF and Y-12 elements where they overlapped in the region of 10.4 inches to 14.4 inches from the center. In this region, the WAFF elements sustained approximately twice the corrosion loss of Y-12 elements. An analysis of weight loss as a function of core radius and sector location showed little variation between similarly spaced elements in different sectors.

The effect of the hot buffer periphery appeared beneficial in reducing corrosion weight loss to elements immediately adjacent to the hot buffer. Weight losses averaged 18.7 gram/element for first row hot buffer elements and 24.9 grams/element for first row normal buffer elements. The hot buffer appeared to provide no significant advantage for second row elements, which averaged weight losses of 22.6 and 22.1 grams/element for hot buffer and nominal buffer zones, respectively.

The relationship of fuel element weight loss versus core radius is shown in Figure 29 for NRX/EST and NRX-A5 reactors.

#### 1.0 Incremental Weight Loss

Incremental weight loss data was obtained upon 66 fuel elements. Weight loss data included that from elements of three regions of the core; twenty-one elements from the central region, twenty-four elements from the core mid-radial region and twenty-one elements from the core periphery. The majority of incremental weight loss data was taken on 1 inch samples; however, some 5 inch flexure samples were also included in the analysis. The data indicated that the integrated weight loss was highest in fuel elements removed from the

~~CONFIDENTIAL~~

**CONFIDENTIAL**

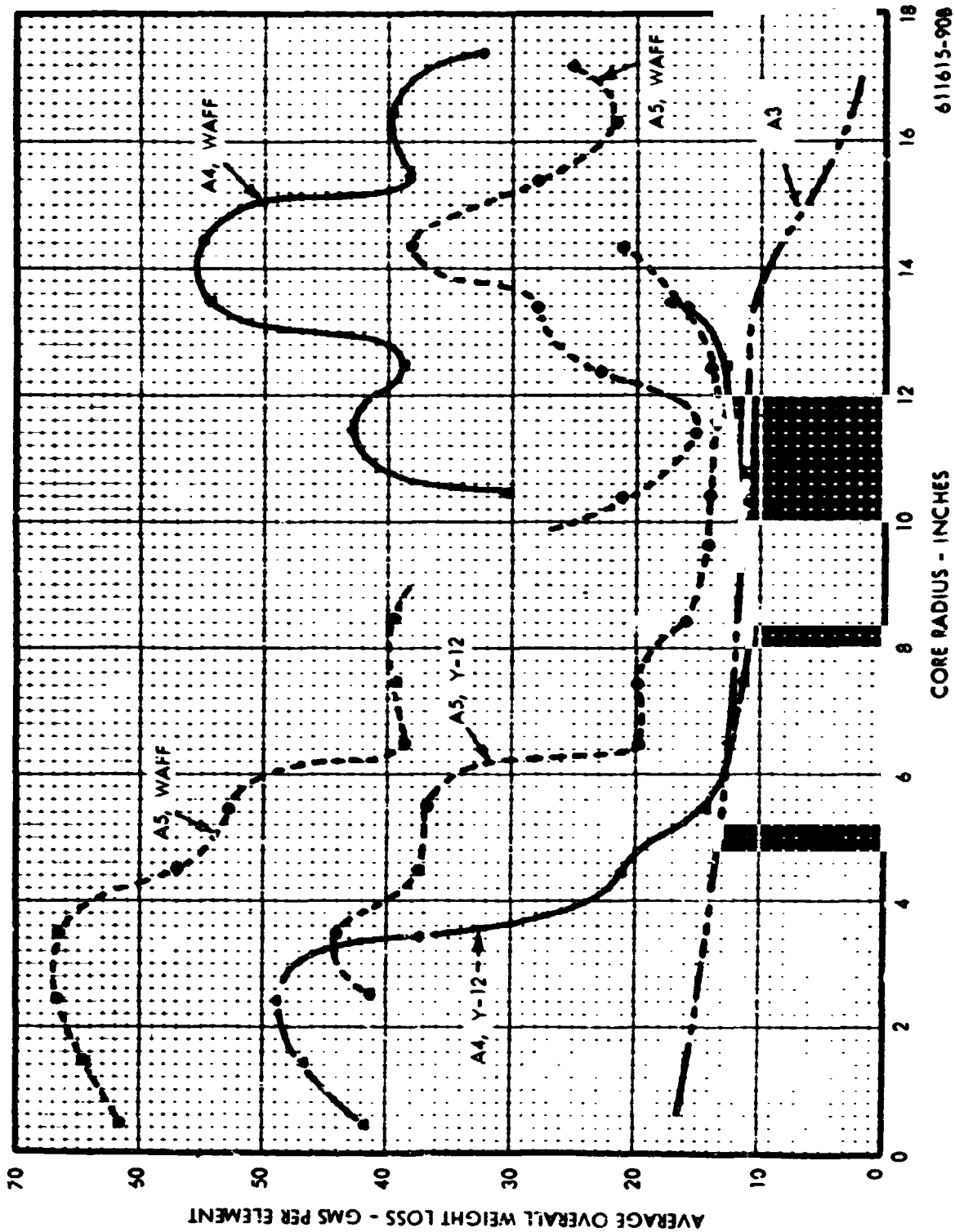


Figure 29. Fuel Element Weight Loss Versus Core Radius

611615-908

**CONFIDENTIAL**

~~CONFIDENTIAL~~



central region and lowest in the mid-radial region. In addition, a well defined peak mid-band weight loss occurred at approximately Station 20 for all elements examined from all regions. A lower hot-end weight loss was noted for NRX-A5 in regions from 30 to 52 inch than was observed on NRX/EST elements. The shape of weight losses was similar for both Y-12 and WAFF elements, although weight losses on WAFF elements was considerably greater.

A summary of the NRX-A5 incremental weight losses for elements examined from the three above locations is shown graphically in Figure 30.

## 2.0 External Surface Weight Loss

Post-test external surface measurements were taken on approximately 127 selected NRX-A5 fuel elements. The data was taken by a measuring device consisting of an LVDT\* connected to a mechanically driven stylus. The data was recorded with a digitized system employing paper tape. Based on the surface regression measurements and on calculated bore coating losses the following were determined: (1) surface weight loss was considerably higher for elements examined from the center of the core than for elements examined from other regions; (2) approximately 15 to 30 percent of the measured core weight loss was due to surface corrosion; (3) the axial distribution of surface weight loss for an element was considerably different than that of bore weight loss, with the majority of the surface corrosion on the outermost row of fuel elements in NRX-A5. The trace data for elements from the hot buffer region showed a reduction in the amount of surface corrosion over elements from the nominal buffer region for the limited number of samples analyzed. The estimated division of surface and bore weight losses, for both Y-12 and WAFF elements, is shown on Figure 31.

As in previous reactors, the analytical methods to predict bore and surface corrosion proved inadequate. However, improvements to the THF-B and TDC codes resulted in better corroboration of calculated surface regression data and measured data. A new code, CAPING, was developed for the specific purpose of performing calculations related to the effects of pinhole formation.

---

\*Linear variable differential transformer

~~CONFIDENTIAL~~

**CONFIDENTIAL**

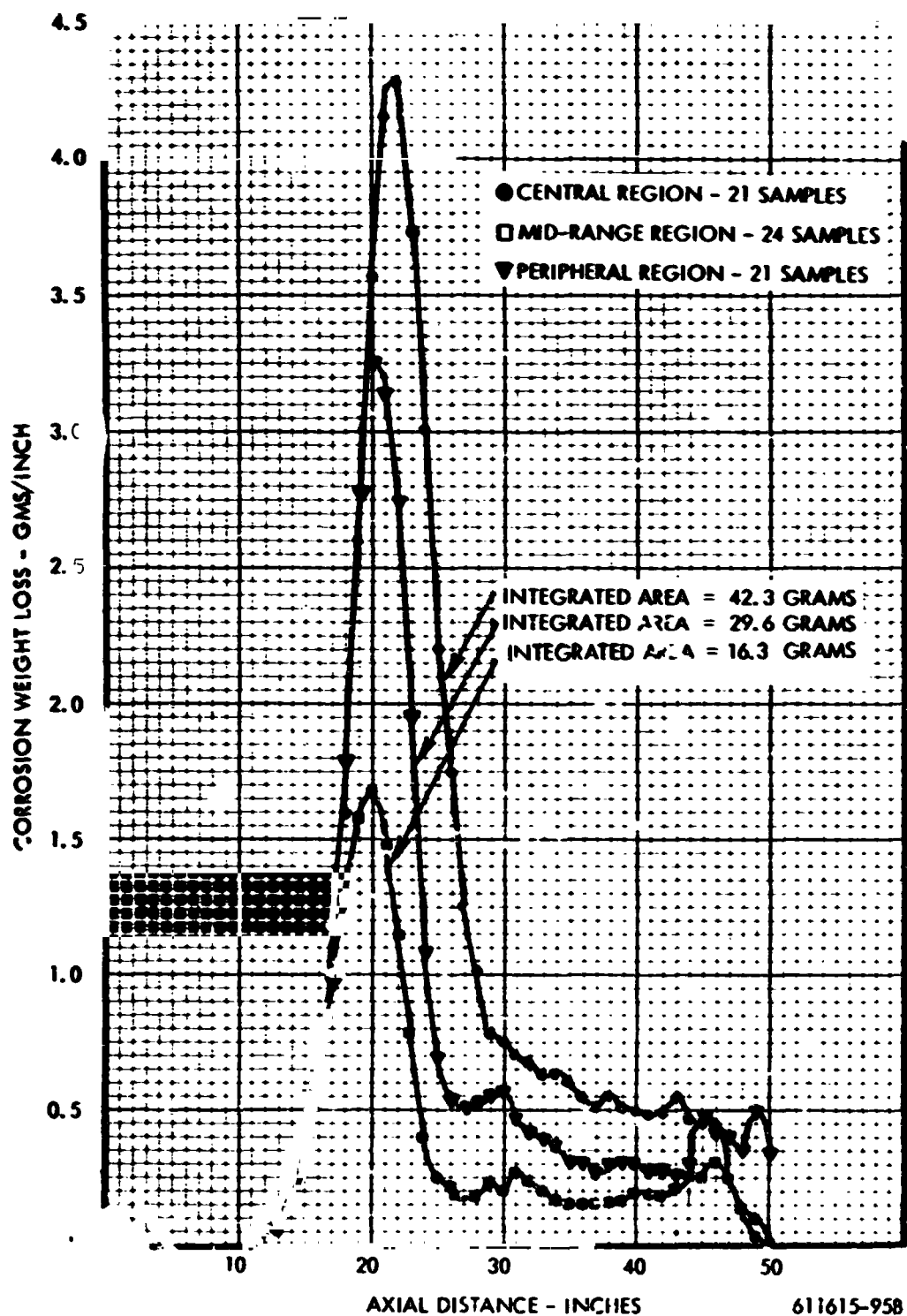


Figure 30. NRX-A5 Incremental Weight Loss

**CONFIDENTIAL**



**CONFIDENTIAL**

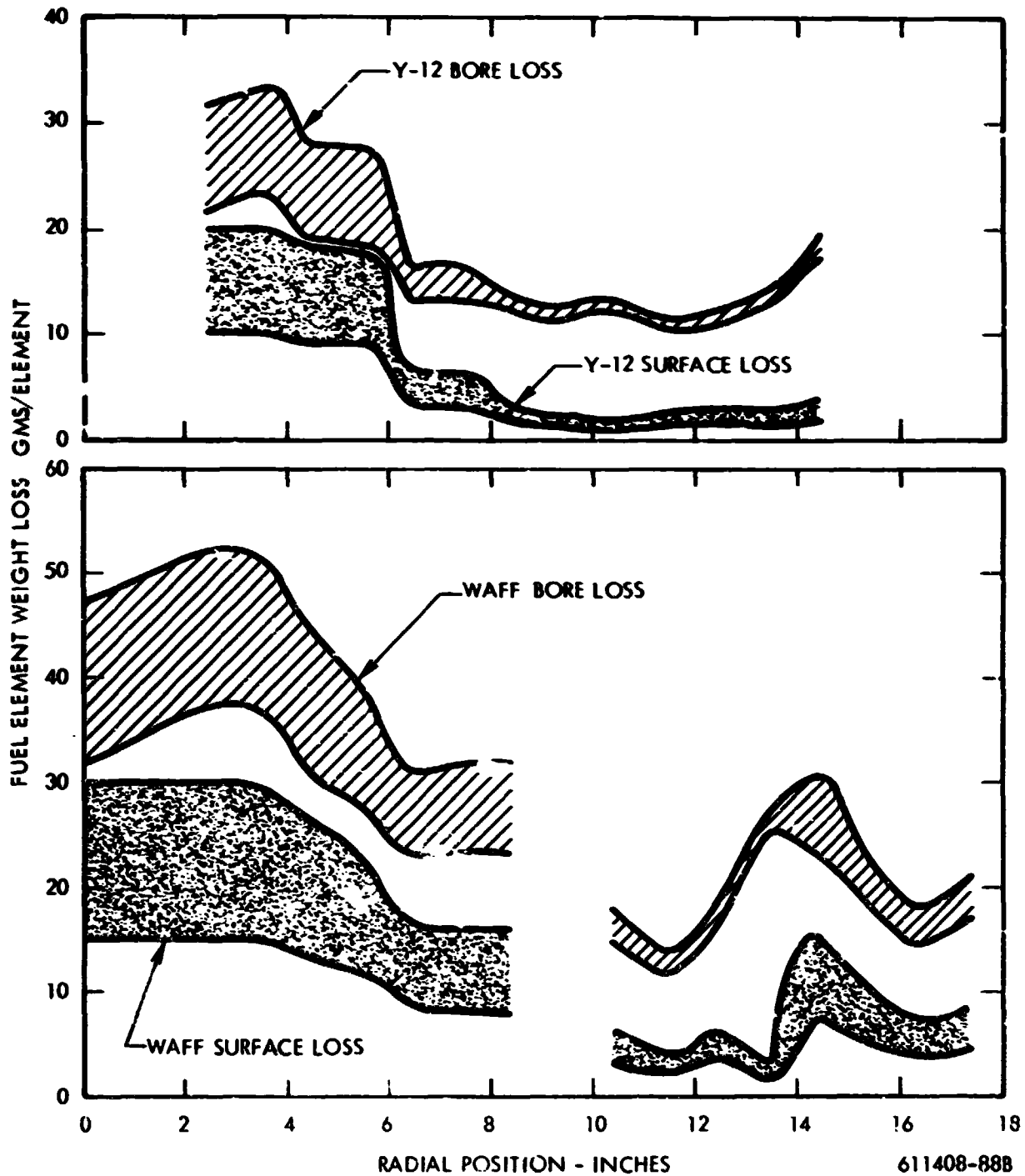


Figure 3I. NRX-A5 Estimated Division of Fuel Element Bore and Surface Weight Loss

**CONFIDENTIAL**



**CONFIDENTIAL****C. PINHOLES AND COOLANT CHANNEL EXPOSURE**

Approximately 1305 NRX-A5 fuel elements were examined for pinholing and channel exposure by analysis of the 70 MM film of faces of each element taken during disassembly. A summary of the results of this examination is presented in Table 3. These elements contained a total of approximately 12,600 pinholes, or an average of about 9.7 pinholes per element.

NRX-A5 WAFF elements averaged 12.5 pinholes per element and Y-12 elements averaged 7.25 pinholes per element. The pinhole density in Y-12 elements remained relatively constant for all sectors except sector 5, where it was approximately twice that of other sectors, probably as a consequence of the previously reported 5F4-5F5 cluster damage. Comparison of NRX/EST and NRX-A5 pinhole data revealed a region of relatively low pinhole density present in both cores at a radius of about 9.0 inches. This region was also the area of low overall weight loss for both NRX/EST and NRX-A5. Compared with NRX/EST, reduction of pinhole damage in the peripheral elements was noted for NRX-A5.

Fuel element coolant channel exposure (fuel beads and matrix are eroded away exposing coolant channel) was recorded for the elements which received pinhole count examination. The study indicated an overall average of approximately 18.6 inches of channel exposure per element. Y-12 elements contained considerably less channel exposure than WAFF elements. Examination of (710) Y-12 elements revealed an average channel exposure of 6.1 inches per element as compared with 33.8 inches per element for 590 WAFF elements examined.

Approximately 1.8 percent (29 elements) of the NRX-A5 core elements exhibited neither pinholes nor coolant channel exposures. Approximately 56 percent of these "zero defect" elements were positioned in the hot buffer region, and most were located in the "J" row. Twelve (12) of the "J" row elements having no observable defects, were externally coated with NbC.

**CONFIDENTIAL**

**Table 3**  
**NRX-A5 Summary Data for Pinholing and Channel Exposure of Fuel Elements Examined**

PINHOLING									
Sector	WAFF ELEMENTS			Y-12 ELEMENTS			WAFF Plus Y-12		
	Pinholes + Holes	Number of Elements	Pinholes Per Element, Sector	Pinholes + Holes	Number of Elements	Pinholes Per Element, Sector	Pinholes/Element, Sector	Pinholes/Element, Sector	
0	58	5	11.6	---	---	---	---	11.6	
1	2171	114	19.06	685	117	5.85	---	12.36	
2	761	102	7.46	609	117	5.20	---	6.25	
3	937	104	9.0	818	120	6.83	---	7.84	
4	995	115	8.65	775	117	6.63	---	7.64	
5	1199	75	16.0	1571	120	13.1	---	14.2	
6	1416	88	16.1	624	111	5.62	---	10.25	
TOTALS	7537	603	Avg. 12.5	5082	702	Avg. 7.25	---	9.67	Avg. of Core
CHANNEL EXPOSURE									
Sector	WAFF ELEMENTS			Y-12 ELEMENTS			WAFF Plus Y-12		
	Inches of Channels Exposed	Number of Elements	Inches of CE/Element, Sector	Inches of Channels Exposed	Number of Elements	Inches of CE/Element, Sector	Inches of CE/Element Sector	Inches of CE/Element Sector	
0	294	4	73.5	---	---	---	---	73.5	
1	2788	114	26.2	183	114	1.61	---	13.9	
2	3670	97	37.85	608	128	4.75	---	19.0	
3	4774	103	46.2	642	118	5.44	---	24.47	
4	3540	113	31.35	1138	118	9.64	---	20.25	
5	2225	73	30.5	1429	123	11.6	---	18.66	
6	2463	86	28.7	333	109	3.06	---	14.32	
TOTALS	19954	590	Avg. 33.8	4333	710	A. J. 6.1	---	18.7	Avg. of Core

**CONFIDENTIAL**

**CONFIDENTIAL**

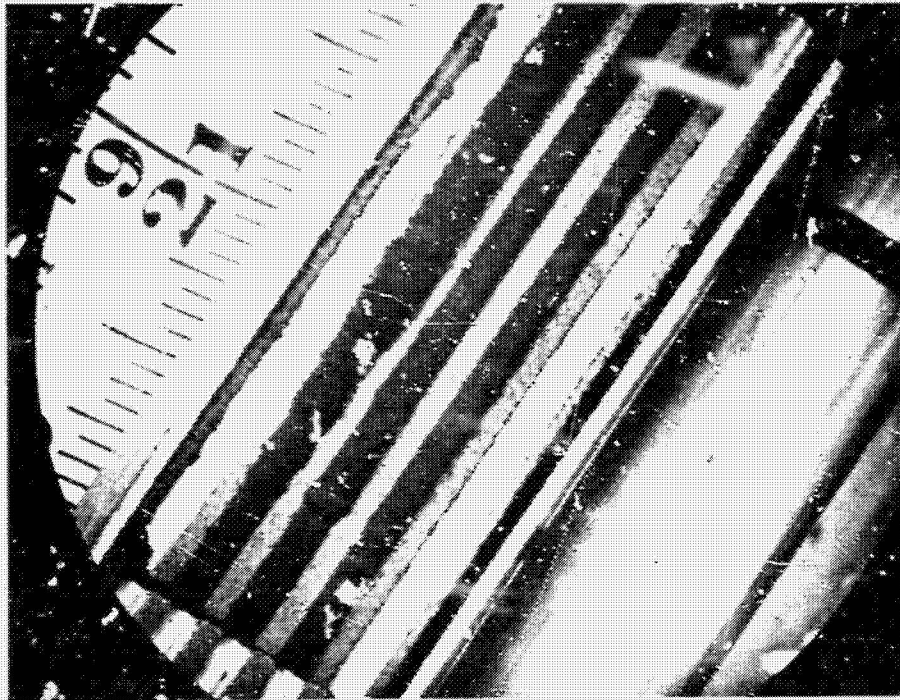


Figure 32. Comparison of Axially Sectioned Adjacent Elements

**CONFIDENTIAL**

~~CONFIDENTIAL~~



D. HOT END CORROSION

Visual examinations were performed and photographs were obtained of the hot ends of all NRX-A5 fuel elements. The hot ends of these elements differed from those of NRX/EST, primarily, in the increased coating length and decreased depth of the undercut after coating. In general, condition of all fuel element hot ends was excellent, with hot ends showing little or no evidence of corrosion.

E. MOLYBDENUM OVERCOATING

The NRX-A5 Core contained two (2) molybdenum bore coated fuel elements. 3J9R in the hot buffer region and 6J8B in the nominal buffer zone. Both elements were broken during attempts to remove them from the core, the breaks occurred at approximately Stations 21 to 22. Weight losses were 12.3 grams for 3J9-R and 16.3 grams for 6J8-B. Weight losses for non-molybdenum coated adjacent elements ranged from 13.6 to 75.0 and 12.0 to 56.0 grams for elements from clusters 3J9 and 6J8, respectively. Surface corrosion and channel exposure was observed on both molybdenum overcoated elements, with at least some of the surface corrosion on the experimental elements due to leakage from adjacent elements.

The weight losses of the molybdenum coated elements were significantly lower than the weight losses of the majority of the adjacent elements in the same clusters. Also, comparison of corrosion on axially sliced elements from the same core region suggests that the molybdenum coating may have been beneficial in reducing midband bore corrosion (see Figure 32).

An additional factor suggesting improvement of the molybdenum overcoated elements was the relative weight loss of these elements with respect to other elements from the same bore coating batch (M-32) as shown by Figure 33. Since the elements of that batch were distributed at different core radii, it was necessary to plot the overall average core weight loss for WAFF elements in this core region. It can be seen from Figure 32 that the weight losses of the non-molybdenum coated elements were generally higher than the core average, while the weight losses of the two molybdenum coated elements were considerably lower than the core average.

~~CONFIDENTIAL~~

~~CONFIDENTIAL~~

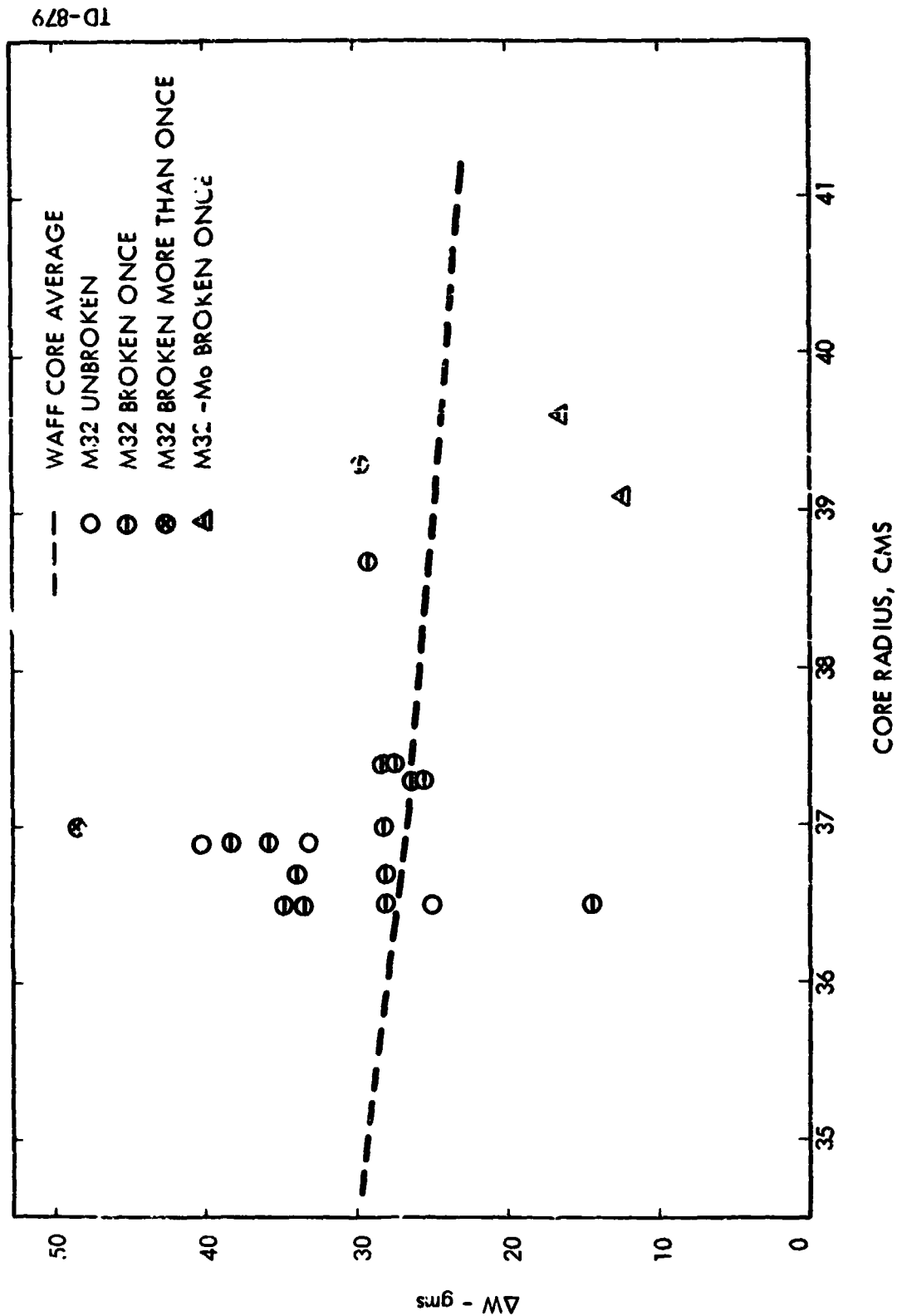


Figure 33. NRX-A5, ΔW "Versus Radius For Batch M-32

~~CONFIDENTIAL~~

~~CONFIDENTIAL~~



It should be stressed that the extremely small sampling of molybdenum coated elements, and the uncertainties with regard to local reactor environment on corrosion behavior preclude full assessment of molybdenum overcoating performance.

~~CONFIDENTIAL~~

**BLANK PAGE**

## VIII. BIBLIOGRAPHY

1. WANL-TNR-176, "NERVA Program NRX-A1 Test Final Report", Test Engineering, September, 1964, CRD.
2. WANL-TNR-193, "NERVA Program NRX-A2 Test Final Report", Test Engineering, March, 1965, CRD.
3. WANL-TNR-210, "NRX-3 Final Report", Test Engineering, December, 1965, CRD.
4. NJD-8, "NERVA NRX-EST Final Report (U)", AGC-REON, WANL, October, 1966, CRD.
5. WANL-TNR-204, "NERVA Program NRX-A5 Test Specification", Test Engineering, February, 1966.
6. WANL-TME-1452, "Development of Drum Limit for NRX-A5 EP-IV Presentation to SNPO-C", 20 June, 1966.
7. WANL-TME-1389, "NRX-A5 Reactor Analysis Data", Thermal and Nuclear Design Department, April, 1966, CRD.
8. WANL-TME-1517, "NRX-A5 Control Systems Design and Evaluation Report", Control Systems Design and Analysis Department, September, 1966, CRD.
9. NTO-R-0071, "NRX-A5 Integrated Nuclear Instrumentation System", E. H. Brooks, NRX Data Group, NERVA Test Operations, May, 1966.
10. NTO-I-0084-I, "Control Room Operating Procedure for NRX-A5 Initial Criticality and Flow Tests, Experimental Plan I, NRX-A5 Test Series", NRX Test Planning, May, 1966.
11. NTO-R-0075, "NRX-A5 Pre-Test Report", NERVA Test Operations, May, 1966.
12. WANL-TME-1388, "NRX-A5 Test Prediction Report", Thermal and Nuclear Design Department, April, 1966, and Supplement No. 1.
13. NTO-I-0084-II, "Control Room Operating Procedure, Simulated Power Test, Neutronics Calibration Adjustments, Experimental Plan II, NRX-A5 Test Series", NRX Test Planning, June, 1966.
14. WANL-TME-1556, "Comparison of the Common Analog Model (CAM) with Transient and Frequency Response Test Data from NRX-A5", S. Goldberg, J. McElhoney, G. H. Steiner, and T. F. Wolsko, May, 1967, CRD.
15. NTO-I-0084-III "Control Room Operating Procedure First Power Test, NRX-A5 Test Series, Experimental Plan III", NRX Test Planning, June, 1966.



16. NTO-I-0084-IV, "Control Room Operating Procedure Second Power Test, NRX-A5 Test Series, Experimental Plan IV", NRX Test Planning, June, 1966.
17. NTC-I-0084-V, "Control Room Operating Procedure Third Full Power Test NRX-A5 Test Series, Experimental Plan V", NRX Test Planning June, 1966.
18. WANL-TNR-219, "NRX-A5 Reactor Test Analysis Report, Thermal and Nuclear Design Department, March, 1967, CRD.
19. NTC-R-0093, "NRX-A5 Chemical and Radiochemical Measurement Report", NTO MAD Operations Radiochemistry Section, September, 1966, CRD.
20. WANL-TME-1519, "WANEF Critical Experiments in Support of NERVA", F. S. Frantz, September, 1966.
21. WANL-TNR-202, "NRX-A3 Reactor Final Test Report", Reactor Analysis Department, December, 1965, CRD.
22. WANL-TME-1575, "NRX-A5 Post-Operative Data Analysis", P. A. Stancampiano, March, 1967, CRD.
23. WANL-TME-1581, "NRX-A5 Post-Operative Mechanical Component Evaluation", R. M. Saccocio, March, 1967, CRD.
24. NTO-R-0076, "EP-I Test Report, NRX-A5 Test Series, Initial Criticality Neutronics Calibration, Control Drum Worth Measurements and Flow Tests", NERVA Test Operations, June, 1966.
25. NTO-R-0078, "EP-II and III Test Report, NRX-A5 Test Series, First Power Test", NERVA Test Operations, June, 1966.
26. NTO-R-0080, "EP-IV Test Report, NRX-A5 Test Series, Second Power Test", NERVA Test Operations, June, 1966.
27. NTO-R-0084, "NRX-A5 Site Test Report", NERVA Test Operations, July, 1966.
28. WANL-TME-1413, "NRX-A5, Safety Evaluation Report", Safeguards Engineering, April, 1966, CRD.
29. WANL-TNR-204, "NRX-A5 Test Specification, Volume II, Section E, Post-Operational Examinations", Test Engineering, April, 1966, CRD.
30. WANL-TME-1423, "Stress Analysis: NRX-A5", A. G. Eggers, May, 1966, CRD.
31. WANL-TME-1301, "Preliminary NRX-A5 Control Systems Predictions (U)", J. M. Walsh and J. Josephson, September, 1965.

32. WANL-TME-1417, "NRX-A5 Test Parameter Limits Justification", J. A. Christenson, Test Operational Planning, May, 1966.
33. NTO-I-0083, "Support Operational Requirements Document, NRX-A5 Test Series", NRX Test Planning, May, 1966.
34. WANL-TME-1383, "NRX-A5 Operating Limits Document", E. H. Hemmerle, Supervisor, Safeguards Engineering, March, 1966.
35. WANL-TME-1383, Revision 1, "NRX-A5 Operating Limits Document", E. H. Hemmerle, Supervisor, Safeguards Engineering, March, 1966.
36. WANL-TME-1383, Revision 2, "NRX-A5 Operating Limits", E. H. Hemmerle, Supervisor, Safeguards Engineering, April, 1966.